

# MinerU2.5-Pro: Pushing the Limits of Data-Centric Document Parsing at Scale

Bin Wang<sup>1\*‡</sup>, Tianyao He<sup>1\*</sup>, Linke Ouyang<sup>1\*</sup>, Fan Wu<sup>1\*</sup>, Zhiyuan Zhao<sup>1\*</sup>, Tao Chu<sup>1\*</sup>  
 Yuan Qu<sup>1\*</sup>, Zhenjiang Jin<sup>1\*</sup>, Weijun Zeng<sup>1\*</sup>, Ziyang Miao<sup>1\*</sup>, Bangrui Xu<sup>1\*</sup>, Junbo Niu<sup>1,2\*</sup>  
 Mengzhang Cai<sup>1</sup>, Jiantao Qiu<sup>1</sup>, Qintong Zhang<sup>1,2</sup>, Dongsheng Ma<sup>1</sup>, Yuefeng Sun<sup>1</sup>, Hejun Dong<sup>1</sup>  
 Wenzheng Zhang<sup>1,2</sup>, Jutao Xiao<sup>1</sup>, Jiayong Shi<sup>1</sup>, Pengyu Liao<sup>1</sup>, Xiaomeng Zhao<sup>1</sup>, Huaping Zhong<sup>4</sup>  
 Liqun Wei<sup>1</sup>, Jing Yu<sup>1</sup>, Jie Yang<sup>1</sup>, Wei Li<sup>1</sup>, Shasha Wang<sup>1</sup>, Qianqian Wu<sup>1</sup>, Xuanhe Zhou<sup>1,3</sup>  
 Weijia Li<sup>1</sup>, Zhenxiang Li<sup>1</sup>, Zhongying Tu<sup>1</sup>, Jiang Wu<sup>1</sup>, Lijun Wu<sup>1</sup>, Chao Xu<sup>1</sup>, Kai Chen<sup>1</sup>  
 Wentao Zhang<sup>1,2</sup>, Yu Qiao<sup>1</sup>, Bowen Zhou<sup>1</sup>, Dahua Lin<sup>1</sup> , Conghui He<sup>1</sup> 

<sup>1</sup>Shanghai Artificial Intelligence Laboratory, <sup>2</sup>Peking University, <sup>3</sup>Shanghai Jiao Tong University, <sup>4</sup>SenseTime

Current document parsing methods compete primarily on model architecture innovation, while systematic engineering of training data remains underexplored. Yet SOTA models of different architectures and parameter scales exhibit highly consistent failure patterns on the same set of hard samples, suggesting that the performance bottleneck stems from shared deficiencies in training data rather than architecture itself. Building on this finding, we present MinerU2.5-Pro, which advances the state of the art solely through data engineering and training strategy optimization while keeping the 1.2B-parameter architecture of MinerU2.5 completely fixed. At its core is a Data Engine co-designed around coverage, informativeness, and annotation accuracy: Diversity-and-Difficulty-Aware Sampling expands training data from under 10M to 65.5M samples while correcting distribution shift; Cross-Model Consistency Verification leverages output agreement among heterogeneous models to assess sample difficulty and generate reliable annotations; the Judge-and-Refine pipeline improves annotation quality for hard samples through render-then-verify iterative correction. A three-stage progressive training strategy—large-scale pre-training, hard sample fine-tuning, and GRPO alignment—sequentially exploits these data at different quality tiers. On the evaluation front, we fix element-matching biases in OmniDocBench v1.5 and introduce a Hard subset, establishing the more discriminative OmniDocBench v1.6 protocol. Without any architectural modification, MinerU2.5-Pro achieves 95.69 on OmniDocBench v1.6, improving over the same-architecture baseline by 2.71 points and surpassing all existing methods including models with over 200× more parameters.

\* Equal contribution  Corresponding author ‡ Project leader

Correspondence: Conghui He, [heconghui@pjlab.org.cn](mailto:heconghui@pjlab.org.cn)

Code: <https://github.com/opendatalab/MinerU>

Model: <https://huggingface.co/opendatalab/MinerU2.5-Pro-2604-1.2B>

Date: April 7, 2026

## Contents

<b>1</b>	<b>Introduction</b>	<b>3</b>
<b>2</b>	<b>Related Work</b>	<b>4</b>
2.1	Document Parsing Methods . . . . .	4
2.2	Data-Centric AI . . . . .	5
2.3	Document Parsing Evaluation . . . . .	5
<b>3</b>	<b>Data Engine</b>	<b>6</b>
3.1	Diversity-and-Difficulty-Aware Data Sampling . . . . .	6
3.2	Cross-Model Consistency Verification . . . . .	8
3.3	Judge-and-Refine Annotation Pipeline . . . . .	9
3.4	Targeted Expert Annotation . . . . .	9
<b>4</b>	<b>Progressive Training Strategy</b>	<b>10</b>
4.1	Stage 1: Document Parsing Pre-training . . . . .	10
4.2	Stage 2: High-Quality Supervised Fine-Tuning . . . . .	11
4.3	Stage 3: Reinforcement Learning with GRPO . . . . .	11
<b>5</b>	<b>OmniDocBench v1.6</b>	<b>12</b>
5.1	Motivation . . . . .	12
5.2	Multi-Granularity Adaptive Matching . . . . .	13
5.3	Hard Subset and Three-Tier Evaluation Protocol . . . . .	14
<b>6</b>	<b>Experiments</b>	<b>14</b>
6.1	Evaluation Setup . . . . .	14
6.2	End-to-End Document Parsing . . . . .	14
6.3	Element-Specific Parsing . . . . .	16
<b>7</b>	<b>Conclusion</b>	<b>17</b>
<b>A</b>	<b>Prompt Design and Task Examples</b>	<b>23</b>
A.1	Layout Detection . . . . .	23
A.2	Text Recognition . . . . .	24
A.3	Formula Recognition . . . . .	24
A.4	Table Recognition . . . . .	24
A.5	Image-Aware Parsing . . . . .	25
<b>B</b>	<b>Extended Parsing Capabilities</b>	<b>25</b>
<b>C</b>	<b>OmniDocBench v1.6 Detailed Results</b>	<b>27</b>
C.1	Detailed Results on Base Subset . . . . .	27
C.2	Detailed Results on Hard Subset . . . . .	27
<b>D</b>	<b>Qualitative Comparison with SOTA Methods</b>	<b>27</b>
D.1	Table Recognition . . . . .	28
D.2	Formula Recognition . . . . .	28
D.3	Image-Aware Parsing . . . . .	28

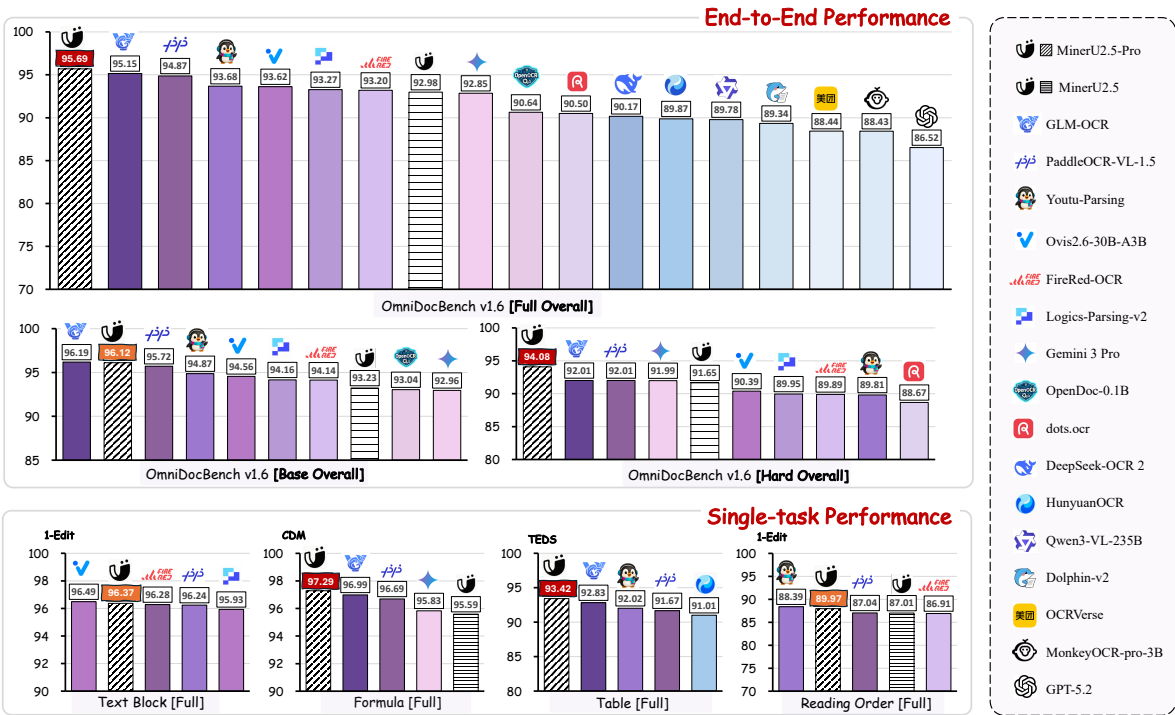


Figure 1: Performance comparison on OmniDocBench v1.6 Base/Hard/Full. Built upon MinerU2.5 with its 1.2B-parameter architecture entirely unchanged, MinerU2.5-Pro improves the overall score from 92.98 to 95.69 solely through data engineering and training strategy optimization, outperforming both specialized document parsing models (e.g. GLM-OCR, PaddleOCR-VL-1.5, Youtu-Parsing) and general-purpose VLMs (e.g. Gemini 3 Pro, Qwen3-VL-235B). Detailed results are presented in Table 2.

# 1 Introduction

Document parsing converts unstructured documents such as PDFs into structured, machine-readable formats (e.g. Markdown), serving as critical infrastructure for LLM training data pipelines [49, 29, 35] and retrieval-augmented generation systems [15, 37, 48]. As end-to-end approaches based on vision-language models (VLMs) progressively replace traditional pipeline systems [2, 39, 25], research has focused predominantly on architectural innovation and inference efficiency optimization, driving rapid score convergence among leading models on standard benchmarks.

Yet this convergence raises a deeper question: what constitutes the remaining performance bottleneck? Our cross-analysis of parsing results from multiple SOTA models—spanning different architectures and parameter scales—on large-scale real-world PDFs reveals a striking pattern: these models exhibit highly similar failure modes on the same hard samples, with certain parsing errors shared across all tested systems. Since these systematic failures transcend any particular architecture, they point to a common root cause: the current performance bottleneck in document parsing stems primarily from shared deficiencies in training data, not from model architecture itself.

This data bottleneck manifests in two interrelated dimensions. First, *insufficient coverage*: taking MinerU2.5 as an example, its training data totals less than 10M pages with distributions concentrated on high-frequency categories, severely underrepresenting long-tail scenarios such as complex nested tables and dense formula layouts. Second, an *annotation quality paradox*: the hard samples that contribute most to model improvement—data that no mainstream model can consistently parse correctly—are precisely those for which automatic annotation is least reliable. Structural annotations for

complex tables and  $\text{\LaTeX}$  transcriptions of dense formulas are highly error-prone, and this annotation noise propagates directly into model behavior during supervised fine-tuning. These two issues are deeply intertwined: simply scaling data volume cannot break through the performance ceiling, as added data only amplifies existing distribution biases and annotation noise.

This cross-analysis also reveals blind spots in the existing evaluation framework. OmniDocBench v1.5 contains relatively few hard samples, and its element-matching logic exhibits systematic preferences for specific output formats, introducing scoring artifacts that complicate fair cross-system comparison. We accordingly introduce OmniDocBench v1.6, which corrects these matching biases and incorporates a dedicated Hard subset to establish a Base/Hard/Full three-tier evaluation protocol.

Based on this analysis, we argue that as model architectures mature, systematic data engineering becomes the primary lever for advancing document parsing performance. To test this hypothesis, we build MinerU2.5-Pro—retaining the identical 1.2B-parameter decoupled coarse-to-fine architecture of MinerU2.5 [25] and focusing all optimization on the Data Engine and training strategy, ensuring that all performance gains are attributable to data-level improvements. On OmniDocBench v1.6, MinerU2.5-Pro achieves 95.69 (baseline 92.98, +2.71), surpassing all existing methods without any architectural modification.

Our contributions are summarized as follows:

- A Data Engine co-designed around coverage, informativeness, and annotation accuracy. It comprises three core components—Diversity-and-Difficulty-Aware Sampling (DDAS), Cross-Model Consistency Verification (CMCV), and a Judge-and-Refine annotation pipeline—that together expand training data from under 10M to 65.5M pages while systematically improving annotation quality through a closed-loop progression from sampling to refinement.
- A three-stage progressive training strategy—large-scale pre-training, high-quality hard sample fine-tuning, and GRPO format alignment—matched to the data quality tiers produced by the Data Engine. With these data and training improvements alone, a 1.2B-parameter model achieves 95.69 on OmniDocBench v1.6, surpassing all existing methods without any architectural modification.
- OmniDocBench v1.6, an upgraded evaluation protocol that corrects element-matching biases in v1.5 through Multi-Granularity Adaptive Matching and introduces a Hard subset, establishing a Base/Hard/Full three-tier framework for fairer and more discriminative evaluation.

## 2 Related Work

### 2.1 Document Parsing Methods

Existing document parsing methods fall into three paradigms based on their overall system architecture.

**Pipeline-based methods.** These methods decompose document parsing into independent subtasks—layout detection, text recognition, table extraction, formula recognition—and execute them in a cascade [35, 50, 21, 28, 7]. This modular design enables independent optimization of each component but is prone to error propagation across stages and information loss between modules.

**End-to-end VLM methods.** These methods directly map document images to structured output, circumventing cascading errors. Nougat [2], built on the Donut architecture [16], established a strong baseline for the image-to-markup paradigm on academic documents; GOT-OCR 2.0 [39] unified scene text and document OCR within a single model. Subsequent works such as Ocean-OCR [3],

olmOCR [29], and dots.ocr [18] employ native-resolution visual encoders to further improve performance. However, native-resolution processing incurs  $\mathcal{O}(N^2)$  token complexity, creating efficiency bottlenecks on high-resolution documents.

**Decoupled VLM methods.** These methods separate layout analysis from content recognition, combining the controllability of pipeline approaches with the semantic modeling power of VLMs. Early works such as Dolphin [12] and MonkeyOCR [19] demonstrated the viability of this paradigm but face limitations in resolution handling or system complexity. MinerU2.5 [25] unifies layout analysis and content recognition within a single model while supporting native-resolution parsing [26], achieving a favorable balance among resolution fidelity, computational efficiency, and deployment complexity at a 1.2B parameter scale. Subsequent works extend the decoupled paradigm along various axes: multi-token prediction for throughput [11], diffusion-based decoding for improved parsing efficiency and robustness [9], non-planar document handling [8], in-the-wild robustness [32], and high-compression vision-text mappings [40]. General-purpose VLMs such as Gemini-2.5 Pro [5] and Qwen2.5-VL-72B [1] also achieve competitive results, though their large parameter scales hinder cost-effective deployment at production scale.

Across these works, the main line of methodological evolution focuses on architecture design and inference efficiency, while systematic engineering of training data—co-optimizing coverage, informativeness, and annotation accuracy—has not been adequately explored as an independent research problem. Our work addresses this dimension and is largely complementary to the architectural advances above.

## 2.2 Data-Centric AI

Data-Centric AI [24, 47] advocates systematically improving data quality while keeping the model fixed, and has been validated in vision-language pretraining [14] and large language model fine-tuning [53]. In document parsing, however, data engineering remains fragmented: olmOCR [29] emphasizes data scale expansion over quality stratification; DocGenome [42] is restricted to academic papers and lacks difficulty differentiation; existing technical reports [25, 11, 8] describe training data but treat it as a prerequisite for model training rather than an independent research subject.

Our work treats data construction for document parsing as a standalone systematic research problem, co-optimizing coverage, informativeness, and annotation accuracy within a unified framework. Methodologically, our CMCV approach draws on the core principles of ensemble-based active learning [30] and query-by-committee [13] by leveraging multi-model disagreement to quantify sample informativeness. Beyond standard disagreement-based selection, CMCV couples difficulty information with downstream annotation strategies in a closed loop and addresses the document-parsing-specific challenge of unreliable hard sample annotation through the Judge-and-Refine pipeline.

## 2.3 Document Parsing Evaluation

Document parsing evaluation involves both metric design and evaluation protocol. At the metric level, text recognition commonly uses edit distance [17], table structure recovery uses TEDS [51], and formula recognition has recently shifted from BLEU to CDM (Character Detection Matching) [36]. OmniDocBench [27] integrates all three metrics and is currently the most comprehensive document parsing evaluation benchmark; OCRBench [20] and CC-OCR [44] focus on evaluating multimodal models' overall OCR capabilities.

At the protocol level, however, the critical impact of element-matching strategies on evaluation fairness remains largely overlooked. End-to-end systems vary in output granularity, segmentation strategies, and format conventions, and the choice of matching algorithm systematically affects evaluation

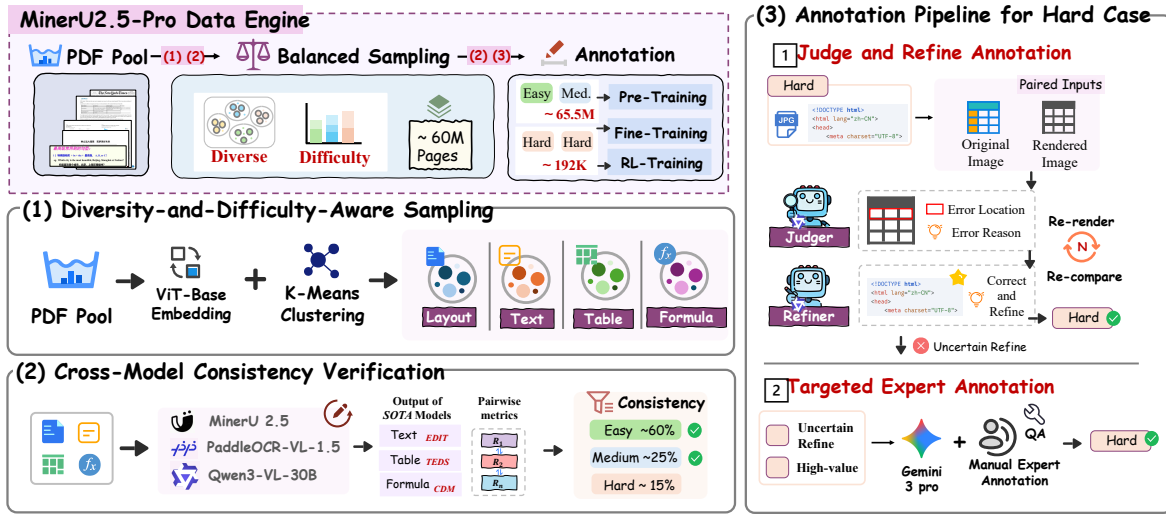


Figure 2: Overview of the Data Engine pipeline. The system co-optimizes three dimensions—Coverage, Informativeness, and Accuracy—through four synergistic stages: Diversity-and-Difficulty-Aware Sampling (DDAS), Cross-Model Consistency Verification (CMCV), Judge-and-Refine annotation correction, and targeted expert annotation.

scores. We identify such systematic biases in OmniDocBench v1.5 and rectify them in v1.6 through Multi-Granularity Adaptive Matching (detailed in Section 5).

### 3 Data Engine

To address the data deficiencies identified above, we first examine the limitations of existing data pipelines. MinerU2.5 [25] built a data pipeline comprising cluster-based sampling, Iterative Model Inference Consistency (IMIC) hard sample mining, and model-based annotation refinement, but these components lack co-design across coverage, informativeness, and accuracy: sampling is not informed by difficulty, annotation refinement applies a uniform strategy regardless of sample difficulty, and hard samples mined by IMIC still face unreliable automatic annotation. Similar limitations exist in PaddleOCR-VL-1.5’s Uncertainty-Aware Cluster Sampling (UACS) [8].

The Data Engine of MinerU2.5-Pro is co-designed around these three dimensions and comprises four synergistic components. DDAS expands data coverage through task-aware clustering and corrects distribution shift (Section 3.1); CMCV performs difficulty stratification on sampled data via multi-model cross-validation, identifying high-informativeness samples (Section 3.2); the Judge-and-Refine pipeline improves annotation accuracy for hard samples through render-then-verify iterative correction (Section 3.3); samples that still exceed automatic correction capability are routed to expert annotation to guarantee final quality (Section 3.4). The four components form a coarse-to-fine quality progression, enabling data scale expansion (under 10M → 65.5M) and annotation quality improvement to proceed in tandem. The overall pipeline is illustrated in Figure 2.

#### 3.1 Diversity-and-Difficulty-Aware Data Sampling

Training data for document parsing faces a typical long-tail distribution problem: high-frequency categories (e.g. standard academic papers, single-column reports) dominate the data pool, while long-tail scenarios such as complex nested tables, dense formula layouts, and unconventional multi-column layouts are severely underrepresented. As noted above, existing approaches [25, 8] rely on

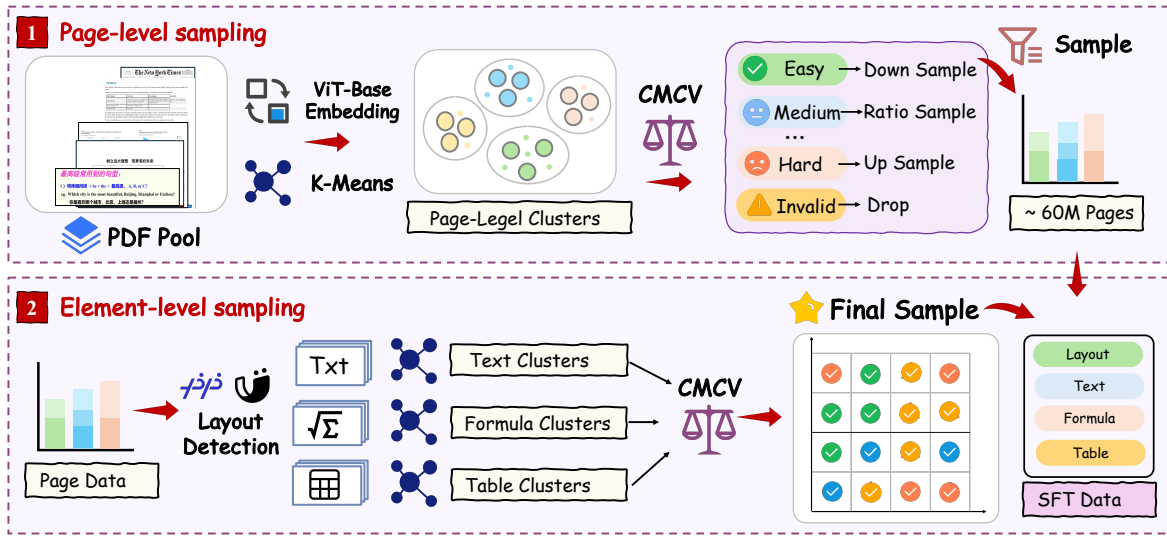


Figure 3: The DDAS pipeline operates at two granularity levels. **Upper:** Page-level sampling for layout detection data—pages from the PDF pool are embedded via ViT-base, clustered, and resampled by jointly weighting cluster diversity and CMCV-derived difficulty, yielding about 60M pages with balanced distribution and difficulty coverage. **Lower:** Element-level sampling—the selected pages are parsed by layout detection models into text, formula, and table blocks; each element type is independently clustered and assessed by CMCV, then sampled to balance both diversity and difficulty at the element granularity. The two levels are combined to produce the final training data for layout, text, formula, and table subtasks.

single-model signals for difficulty estimation, which cannot distinguish model-specific weaknesses from universally hard samples.

We propose Diversity-and-Difficulty-Aware Sampling (DDAS), which jointly optimizes diversity and difficulty at both page-level and element-level granularity. The overall pipeline is shown in Figure 3.

**Stage 1: Page-level sampling.** We extract visual features (ViT-base, 512-dim) from all pages in the PDF document pool, perform K-Means clustering, and uniformly sample from each cluster center to form an initial candidate set. We then run page-level CMCV (Section 3.2) on this candidate set to obtain difficulty labels for each page. Based on statistical analysis of the difficulty distribution within each cluster, we adjust sampling weights: clusters dominated by Easy samples receive lower weight, clusters with diverse difficulty distributions receive higher weight, and clusters dominated by invalid content (non-target languages, blank pages, *etc.*) are filtered out. Using the adjusted weights, we expand sampling from the original document pool to obtain the page-level candidate set and complete page-level CMCV difficulty annotation for all data.

**Stage 2: Element-level sampling.** From the page-level candidate set, we extract block-level elements (text blocks, formula blocks, table blocks) using MinerU2.5 and PaddleOCR-VL layout detection models. For each element type, we extract visual features and perform independent clustering, while simultaneously running block-level CMCV to obtain element difficulty labels. At this point, all four subtasks—layout, text, formula, and table—have complete information along both the clustering (diversity) and CMCV (difficulty) dimensions.

**Final sampling.** We perform balanced sampling in the joint cluster-difficulty space across all four subtasks: along the diversity dimension, large clusters are downsampled and small clusters are upsampled to correct long-tail shift; along the difficulty dimension, the proportions of Medium and Hard samples are upweighted to enhance training signal informativeness. The final output is an SFT training set that covers all subtasks and balances diversity with difficulty.

By coupling clustering with CMCV at both page-level and element-level granularity, DDAS enables sampling decisions to simultaneously account for data distribution and training value, maximizing training signal density while controlling total data volume.

### 3.2 Cross-Model Consistency Verification

DDAS relies on difficulty labels to guide sampling weight allocation, and subsequent annotation refinement and expert annotation also require difficulty information to determine resource investment strategies. However, ground truth is unavailable for massive unlabeled data. IMIC in MinerU2.5 [25] and UACS in PaddleOCR-VL-1.5 [8] use output consistency from multiple inferences of a single model as a difficulty proxy. This paradigm captures only the epistemic uncertainty of a single model and cannot distinguish between model-specific blind spots and universally hard problems—the former can be directly rectified via cross-model consensus, while the latter necessitates additional quality refinement or even human intervention. This distinction is critical for annotation strategy selection.

We propose Cross-Model Consistency Verification (CMCV), which extends difficulty assessment from single-model introspection to multi-model cross-validation. The underlying assumption is empirically validated: when multiple heterogeneous models produce consistent outputs for a given sample, the result is highly likely to be correct; when all models diverge substantially, the sample is genuinely difficult and none of the models can parse it reliably. Based on this assumption, we run  $K$  heterogeneous SOTA document parsing models (MinerU2.5, PaddleOCR-VL, Qwen3-VL-30B) independently on the candidate data produced by DDAS, compute task-specific pairwise consistency metrics (text: edit distance; table: TEDS; formula: CDM), and classify each sample into three difficulty tiers based on consistency patterns. Since MinerU2.5 is the target model to be improved, we anchor the difficulty taxonomy on its performance relative to external models:

- **Easy:** MinerU2.5’s output is highly consistent with at least one external model. Model consensus indicates the parsing result is reliable, and any model’s output can serve directly as annotation.
- **Medium:** The two external models agree with each other, but MinerU2.5 differs significantly from both. The external consensus serves as a reliable pseudo-label.
- **Hard:** All three models’ outputs exhibit significant pairwise disagreement, and no reliable annotation can be obtained through model consensus.

These three data categories play different roles in training. Easy data is abundant and reliably annotated, forming the backbone for building foundational capabilities, but the model has largely mastered these scenarios and their marginal training value is limited. Medium data has the highest training value—it precisely pinpoints MinerU2.5’s capability gaps relative to peers, while the successful parsing by external models proves these samples are learnable, and the external consensus directly provides reliable annotations without further correction. Hard data is critical for capability breakthroughs, but its annotations are unreliable and require subsequent Judge-and-Refine correction (Section 3.3) or expert annotation (Section 3.4) before safe use. The respective strengths and constraints of these three categories naturally motivate the annotation strategy design in the following sections.

CMCV thus enables rapid difficulty assessment on massive unlabeled data without human annotation, making large-scale data expansion and iteration feasible. Since Medium data is scarce but most valuable, we prioritize its proportion during DDAS sampling. The optimal ratio among the three

categories varies by subtask—formula and table recognition are more sensitive to Hard samples, while text recognition benefits more from Medium samples.

### 3.3 Judge-and-Refine Annotation Pipeline

CMCV provides reliable automatic annotations for Easy and Medium samples. However, Hard samples—data on which all models fail to reach consensus—would introduce annotation noise that degrades rather than improves model performance if directly used for training. Improving annotation quality for these critical samples without relying on large-scale human annotation is the core challenge in advancing the Data Engine from “filtering” to “refinement.”

A natural approach is to introduce test-time compute through an iterative judge-then-correct mechanism that lets the model examine and refine its own parsing results. However, naive self-reflection suffers from a form of confirmation bias in document parsing: when a model is asked to check its own output, it tends to accept the result as correct and overlook existing errors. The root cause lies in the asymmetry of cross-modal mapping—models excel at generating structured sequences from document images but struggle to infer visual appearance from structured sequences. For complex structural mappings such as  $\text{\LaTeX}$  formulas and HTML tables, the model cannot accurately judge how an output sequence will render visually in implicit space, losing the ability to detect structural errors.

To break this bottleneck, we incorporate *render-then-verify* into the iterative correction loop: we compile  $\text{\LaTeX}$  formulas and render HTML tables into images, then feed both the original document image and the rendered image to the model as paired inputs alongside the judge-and-refine prompt. This design offers two advantages. First, it fills in the missing mapping from structured text to visual layout, reducing the cognitive load on the model during cross-modal alignment. Second, the error-amplification effect of rendering translates subtle, text-domain structural flaws (*e.g.* missing alignment symbols, unclosed tags) into salient visual anomalies or layout collapse, enabling the model to localize defects as intuitively as a human proofreader.

Based on this design, we build a visual-comparison-driven Judge-and-Refine iterative correction pipeline. The pipeline uses Qwen3-VL-235B as the Judge-Refine model—chosen for its strong multi-modal reasoning capability and its independence from the CMCV model pool, which avoids systematic bias in error detection. Multi-round error localization and targeted correction are driven through direct visual comparison between the original document image and the rendered image. After processing through this pipeline, a subset of extremely complex cases still exceeds automatic correction capability; these samples are routed to the expert annotation workflow.

### 3.4 Targeted Expert Annotation

After DDAS sampling, CMCV difficulty stratification, and Judge-and-Refine correction, Easy and Medium samples have reliable annotations, but a portion of Hard samples still exceeds automatic correction capability. For these samples, we introduce expert human annotation to guarantee final quality. Annotation budget allocation is prioritized based on intermediate outputs from Judge-and-Refine:

1. Samples where Judge confidence is high but Refine correction is uncertain receive top priority—error locations have already been identified by Judge, and annotators need only perform local corrections, maximizing annotation efficiency.
2. Priority is given to the subtask categories where the current model is weakest (determined by CMCV disagreement patterns), maximizing the marginal contribution of limited annotation budget to overall performance.

Human annotation follows an AI pre-annotation and expert review-and-correction workflow. For pre-annotation, we use Gemini 3 Pro—chosen for its strong multimodal reasoning capability and

Table 1: Training configurations for the three-stage progressive strategy. All three stages share the same model architecture and resolution settings; they differ in data source, data scale, and optimization hyperparameters, reflecting the progression from broad coverage (Stage 1) to targeted refinement (Stage 2) to metric-level alignment (Stage 3).

Category	Parameter	Stage 1	Stage 2	Stage 3
Vision	Max Resolution	2048×28×28	2048×28×28	2048×28×28
	#Tokens per Image	64–2048	64–2048	64–2048
Data	Dataset Type	Layout & OCR <sup>†</sup> & Image Analysis	Layout & OCR <sup>†</sup> & Image Analysis	Layout & Text & Formula & Table
	#Samples	65.5M	3.9M (192K human-labeled)	192K
Model	Trainable	All	All	All
	Sequence Length	8192	8192	8192
Training	Batch Size	256	128	512
	ViT Learning Rate	$1 \times 10^{-4}$	$5 \times 10^{-6}$	$1 \times 10^{-7}$
	MLP/LLM Learning Rate	$1 \times 10^{-3}$	$5 \times 10^{-5}$	$1 \times 10^{-5}$
	Epoch	1	1	1

<sup>†</sup>OCR collectively refers to text recognition, formula recognition, and table recognition.

its independence from the CMCV model pool, thereby avoiding data leakage. Automated QA tools further ensure annotation consistency. Compared to MinerU2.5’s human annotation process [25], annotation targets shift from random sampling to a precisely targeted subset identified through three-stage filtering, significantly improving annotation resource utilization.

The Data Engine produces a stratified dataset: approximately 65.5M Easy and Medium samples, automatically annotated via CMCV, are used for Stage 1 pre-training; 192K expert-annotated Hard samples are used for Stage 2 fine-tuning and Stage 3 GRPO alignment.

## 4 Progressive Training Strategy

MinerU2.5-Pro inherits MinerU2.5’s [25] 1.2B-parameter decoupled coarse-to-fine architecture (NaViT-675M vision encoder + Qwen2-0.5B language model) without any structural modification. The model is initialized from MinerU2.5’s Stage 0 checkpoint, which provides foundational vision-language alignment and OCR capabilities [25].

From this shared starting point, MinerU2.5-Pro employs a three-stage progressive training strategy that sequentially leverages data at different quality tiers produced by the Data Engine: Stage 1 pre-trains on large-scale CMCV auto-annotated data to build comprehensive foundational capabilities; Stage 2 fine-tunes on high-quality expert-annotated data to strengthen hard scenarios; Stage 3 aligns output format and structural conventions through reinforcement learning. The three stages progress from data scale to data quality, with training configurations summarized in Table 1.

### 4.1 Stage 1: Document Parsing Pre-training

**Training data.** The training set consists of Easy and Medium samples produced by the Data Engine, with annotations derived from CMCV multi-model consensus. The data covers four core subtasks totaling approximately 65.5M samples: text recognition 21M, layout analysis 14M, formula recognition 13M, and table recognition 11.5M, plus 6M image analysis samples (charts, text-embedded images, etc.). The ratio among subtasks is adjusted based on their weights in the OmniDocBench overall score

and the baseline model’s performance gaps.

**Training configuration.** All parameters are trainable. The language model uses a learning rate of  $1 \times 10^{-3}$ , the vision encoder uses  $1 \times 10^{-4}$ , batch size is 256, and training runs for 1 epoch. Compared to MinerU2.5’s Stage 1 pre-training (6.9M samples/epoch  $\times$  2 epochs) [25], this stage expands data scale by nearly an order of magnitude (6.9M  $\rightarrow$  65.5M), with data quality also systematically improved through DDAS distribution correction and CMCV annotation filtering.

### 4.2 Stage 2: High-Quality Supervised Fine-Tuning

Stage 1 builds comprehensive foundational capabilities, but performance gaps remain on Hard samples. This stage uses high-quality expert-annotated data for precise fine-tuning, strengthening hard scenarios while maintaining generalization on regular scenarios through mixed Stage 1 replay data.

**Training data.** The training set comprises two parts: (1) 192K high-quality Hard samples produced through the expert annotation pipeline; (2) replay data sampled proportionally from the Stage 1 training set to prevent catastrophic forgetting. The mixing ratio (Hard:Replay) is differentiated by subtask: layout analysis 6:1, text recognition 1:50, formula recognition 1:25, table recognition 1:10, and image analysis 1:4. This non-uniform mixing strategy reflects differences in hard sample volume and baseline performance across subtasks—layout analysis has more hard samples and a strong Stage 1 foundation, requiring less replay; text recognition has scarce hard samples and needs more replay data to maintain generalization.

**Training configuration.** Building on the Stage 1 model, we adopt a lower learning rate of  $5 \times 10^{-5}$ , batch size of 128, and train for 1 epoch. The reduced learning rate protects foundational capabilities acquired in Stage 1 while fine-tuning decision boundaries on hard scenarios.

### 4.3 Stage 3: Reinforcement Learning with GRPO

The first two stages optimize content recognition accuracy through supervised learning, but cross-entropy loss optimizes each token prediction independently and weights all tokens equally, without directly reflecting sequence-level or structure-level evaluation metrics (edit distance, CDM, TEDS, IoU). This stage bridges the gap between training objectives and evaluation metrics through reinforcement learning that directly optimizes task-level metrics.

We use Group Relative Policy Optimization (GRPO) [31] for alignment. For each input,  $G$  groups of candidate outputs are sampled, rewards are computed directly using task-specific automatic evaluation metrics, and policy updates are guided by within-group relative advantages, eliminating the need for a separate reward model.

**Reward design.** Reward functions are designed separately for four subtasks, directly adopting the same metrics used in evaluation as reward signals: edit distance for text recognition, CDM for formula recognition, TEDS for table recognition, and category IoU for layout detection. This design directly aligns training optimization objectives with final evaluation metrics.

**Training data.** Training data is generated from Stage 2 model rollouts and filtered based on reward distribution: samples with excessively high rewards (model saturated, no effective learning signal) and excessively low rewards (samples too hard or annotations erroneous) are removed, retaining the mid-reward range to maximize effective policy gradient signal. All training data comes from the high-quality expert-annotated set to ensure reward signal reliability.

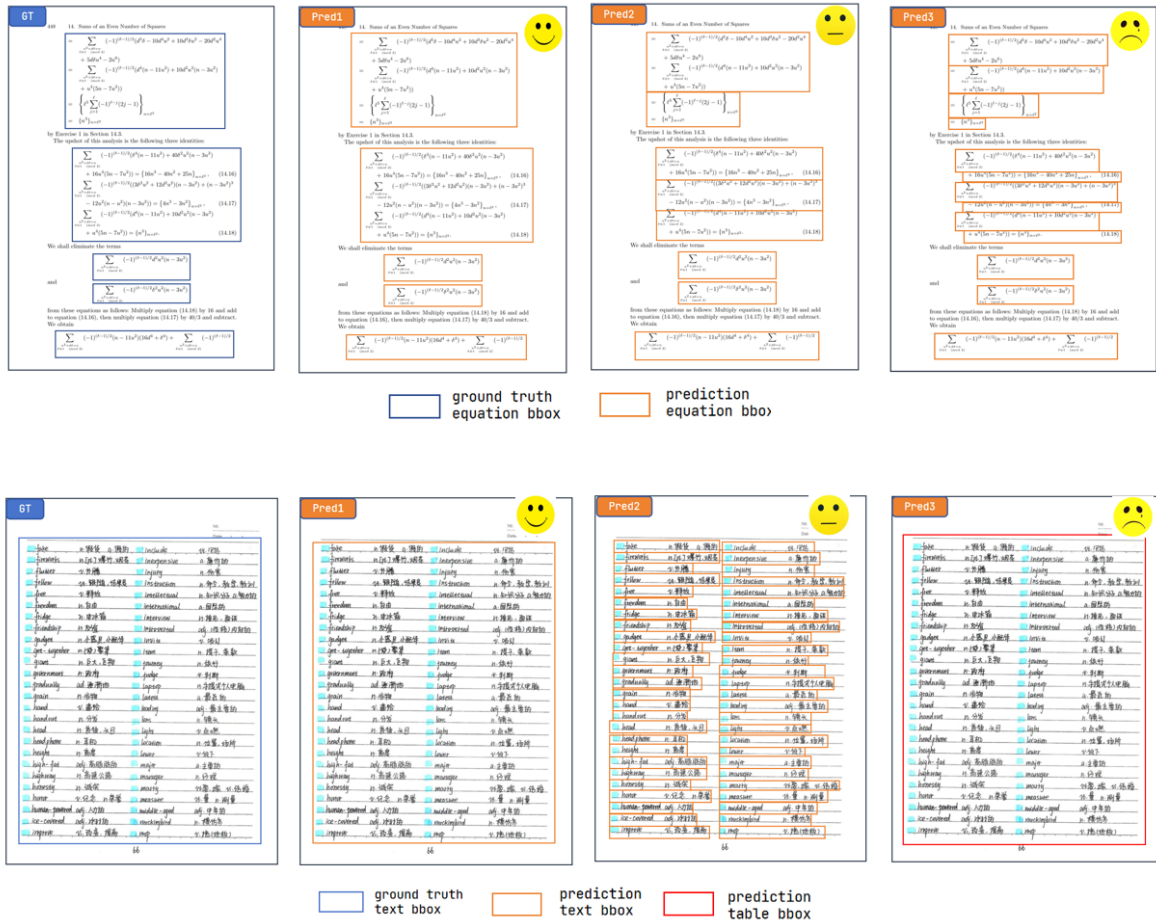


Figure 4: Examples of element-matching bias in OmniDocBench v1.5. Semantically correct predictions receive low scores due to granularity mismatch between predicted and ground-truth segmentation.

**Training configuration.** Building on the Stage 2 model, we adopt a learning rate of  $1 \times 10^{-5}$ , batch size of 512, and train for 1 epoch, with  $G = 16$  rollouts per sample. Following DAPO [46], we apply clip-higher to stabilize advantage estimation and dynamic sampling to discard zero-variance rollout groups.

## 5 OmniDocBench v1.6

### 5.1 Motivation

As leading document parsing models converge on OmniDocBench v1.5, two fundamental issues limit its effectiveness as a benchmark:

**Matching strategy bias.** v1.5 employs fixed-granularity one-to-one element matching, which silently penalizes systems whose output segmentation differs from the ground truth—even when the parsed content is entirely correct. As illustrated in Figure 4, consider a multi-line formula annotated as a single block spanning  $k$  lines: if a model produces the identical L<sup>A</sup>T<sub>E</sub>X but segments it into  $k-1$  or  $k$  separate blocks, v1.5 scores drop sharply from full marks to near zero despite semantically perfect output. A

similar issue affects dense text: a region annotated as one block may be predicted line-by-line or even recognized as a table; in the latter case v1.5 assigns zero credit because no text element remains to match. These granularity-dependent scoring artifacts make cross-system comparisons unreliable.

**Insufficient hard sample coverage.** Through the large-scale difficulty stratification provided by our Data Engine (Section 3), we find that samples labeled as Hard are virtually absent from the v1.5 evaluation set. The benchmark predominantly measures performance on low-to-medium difficulty documents, causing top models to cluster tightly with diminishing discriminative power.

To address these issues, we upgrade OmniDocBench to v1.6: we propose Multi-Granularity Adaptive Matching (MGAM) to eliminate matching bias (Section 5.2), and expand the evaluation set with a dedicated Hard subset (Section 5.3).

## 5.2 Multi-Granularity Adaptive Matching

We propose **Multi-Granularity Adaptive Matching (MGAM)**, which eliminates matching bias through adaptive granularity adjustment on the prediction side. The core principle is to keep the ground truth unchanged and search for the optimal segmentation granularity only on the prediction side. Given a set of ground truth elements  $\mathcal{G} = \{g_1, g_2, \dots, g_m\}$  and prediction elements  $\mathcal{P} = \{p_1, p_2, \dots, p_n\}$ , MGAM generates candidate matching solutions through three stages and selects the global optimum:

**Stage 1: Direct Bipartite Matching.** We directly solve optimal bipartite matching between  $\mathcal{P}$  and  $\mathcal{G}$  at original granularity. Using the cost matrix  $C_{ij} = 1 - \text{sim}(p_i, g_j)$  as input, the Hungarian algorithm solves for the minimum-cost matching  $\mathcal{M}_1^* = \arg \min_{\mathcal{M}} \sum_{(i,j) \in \mathcal{M}} C_{ij}$ , yielding the first candidate matching and its aggregate score  $S_1$ .

**Stage 2: Prediction Splitting + Bipartite Matching.** Each prediction element  $p_i$  is split at  $\text{\LaTeX}$  line-break delimiters (e.g. `\|`, `\newline`, and equivalent symbols) to produce a fine-grained prediction set  $\mathcal{P}' = \{p'_1, p'_2, \dots, p'_{n'}\}$  ( $n' \geq n$ ). Prediction elements without splittable delimiters remain unchanged. Bipartite matching is re-solved on  $\mathcal{P}'$  and  $\mathcal{G}$ , yielding candidate matching  $\mathcal{M}_2^*$  and aggregate score  $S_2$ .

**Stage 3: Partition Enumeration + Bipartite Matching.** Stage 2 splitting may be too fine—annotation granularity is not necessarily per-line but may be any intermediate granularity between 1 and  $k$  lines. To cover all possible merging schemes, we enumerate all valid ordered partitions of consecutive subsequences of  $\mathcal{P}'$ . Specifically, for  $n'$  fine-grained prediction elements, there are  $n' - 1$  gaps between adjacent elements, and each gap can be either “split” or “merged,” producing  $2^{n'-1}$  partition schemes. Each partition  $\pi = (B_1, B_2, \dots, B_K)$  divides  $\mathcal{P}'$  into  $K$  consecutive blocks, where the  $k$ -th block is

$$B_k = \bigoplus_{t=l_k}^{r_k} p'_t \quad (1)$$

with  $\bigoplus$  denoting concatenation in original order. For each partition, we perform bipartite matching between the merged block set  $\{B_1, \dots, B_K\}$  and  $\mathcal{G}$ , selecting the partition with the best matching score as candidate matching  $\mathcal{M}_3^*$  and aggregate score  $S_3$ .

**Global Optimum Selection.** The final matching is the one with the best aggregate score among the three stages:  $\mathcal{M}^* = \arg \max_{k \in \{1,2,3\}} S_k$ , and the task-specific metric (e.g. CDM for formulas, edit distance for text) is computed based on  $\mathcal{M}^*$ .

**Dense text matching.** The granularity mismatch problem is not limited to formulas. For dense text regions, prediction and annotation sides similarly differ in whether multiple text segments are merged into one large text box or split into multiple small ones. We reuse the MGAM algorithm for text elements with edit distance as the similarity metric. Additionally, if a model recognizes text in a region as a table (not uncommon for dense structured text), we convert the table back to plain text and include it in the same matching pipeline, avoiding unfair penalties due to format preference differences.

With MGAM, the evaluation becomes neutral to output granularity and format preferences, removing a systematic source of scoring variance across systems.

### 5.3 Hard Subset and Three-Tier Evaluation Protocol

To fill the coverage gap for hard scenarios, we construct a Hard subset of 296 pages selected from the pool of data labeled as Hard during Data Engine difficulty stratification. Samples are chosen to cover the most challenging scenario categories in document parsing, including complex nested tables, dense mathematical formula layouts, and unconventional layout structures. All Hard subset samples are excluded from every training stage of MinerU2.5-Pro (including Judge-and-Refine training data) and are annotated by professional teams with inter-annotator cross-validation to ensure ground truth quality.

OmniDocBench v1.6 establishes a Base/Hard/Full three-tier evaluation protocol:

- **Base** (1,355 pages): retains the original v1.5 evaluation set to maintain comparability with historical results.
- **Hard** (296 pages): the newly added hard sample subset, providing more sensitive measurement where top models saturate on standard evaluations.
- **Full** (1,651 pages): the complete union of both, providing comprehensive performance assessment.

## 6 Experiments

This section evaluates MinerU2.5-Pro against both leading general-purpose VLMs and current SOTA document-parsing-specific models [5, 43, 33, 11, 8, 32, 41, 40, 25]. All competing models are re-evaluated under a unified environment using the same evaluation code.

### 6.1 Evaluation Setup

**OmniDocBench v1.6.** We evaluate on OmniDocBench v1.6 using the Base/Hard/Full three-tier protocol described in Section 5.3. The overall score follows the same formula as MinerU2.5 [25], averaging text (edit distance), table (TEDS), and formula (CDM) metrics. We additionally report sub-metrics: Text Edit↓, Formula CDM↑, Table TEDS↑, Table TEDS-S↑, Read Order Edit↓.

**Element-specific evaluation.** To more accurately measure content recognition capability (excluding the confounding effect of layout detection errors), we crop document images based on ground truth layout boxes and separately evaluate text recognition, formula recognition, and table recognition as individual modules.

### 6.2 End-to-End Document Parsing

As shown in Table 2, MinerU2.5-Pro ranks first on Full with 95.69, improving over the same-architecture MinerU2.5 baseline (92.98) by 2.71 points—confirming that all gains are data-driven. On the Base

# MinerU2.5-Pro: Pushing the Limits of Data-Centric Document Parsing at Scale

Model Type	Methods	Param	Overall $\uparrow$	Text $\text{Edit}\downarrow$	Formula $\text{CDM}\uparrow$	Table $\text{TEDS}\uparrow$	Table $\text{TEDS-S}\uparrow$	Read Order $\text{Edit}\downarrow$
Specialized VLMs	MinerU2.5-Pro	1.2B	<b>95.69</b>	<b>0.036</b>	<b>97.29</b>	<b>93.42</b>	<b>95.92</b>	<b>0.120</b>
	GLM-OCR [11]	0.9B	95.15	0.044	96.99	92.83	95.39	0.133
	PaddleOCR-VL-1.5 [8]	0.9B	94.87	0.038	96.69	91.67	94.37	0.130
	PaddleOCR-VL [6]	0.9B	94.11	0.040	95.70	90.65	93.74	0.135
	Youtu-Parsing [45]	2.5B	93.68	0.044	93.45	92.02	95.00	<b>0.116</b>
	Logics-Parsing-v2 [4]	4B	93.27	0.041	95.47	88.42	91.98	0.137
	FireRed-OCR [41]	2B	93.20	0.037	95.27	88.04	91.06	0.131
	MinerU2.5 [25]	1.2B	92.98	0.045	95.59	87.88	91.47	0.130
	OpenDoc-0.1B [10]	0.1B	90.64	0.049	92.93	83.88	87.45	0.140
	dots.ocr [18]	3B	90.50	0.048	89.12	87.18	90.58	0.138
	DeepSeek-OCR 2 [40]	3B	90.17	0.050	91.59	83.89	87.75	0.144
	HunyuanOCR [32]	1B	89.87	0.089	87.44	91.01	93.23	0.171
	Dolphin-v2 [12]	3B	89.34	0.069	90.53	84.40	87.44	0.150
	OCRVerse [52]	4B	88.44	0.063	89.14	82.44	86.27	0.163
	MonkeyOCR-pro-3B [19]	3B	88.43	0.074	88.33	84.35	88.62	0.189
General VLMs	Ovis2.6-30B-A3B [22, 23]	30B	93.62	<b>0.035</b>	94.93	89.44	92.40	0.135
	Gemini 3 Pro	-	92.85	0.064	95.83	89.15	92.96	0.165
	Gemini 3 Flash	-	92.58	0.066	95.03	89.29	93.51	0.173
	Qwen3-VL-235B [43]	235B	89.78	0.063	92.53	83.07	86.75	0.166
	GPT-5.2	-	86.52	0.114	88.00	82.95	87.93	0.193
	InternVL3.5-241B [38]	241B	83.61	0.130	89.52	74.35	79.78	0.215

Table 2: Performance comparison of document parsing methods on OmniDocBench v1.6 Full across text, formula, table, and reading order extraction tasks.

Table 3: Training stage ablation on OmniDocBench v1.6.

Stage	Base	Hard	Full	$\Delta\text{Full}$	Text $\downarrow$	CDM $\uparrow$	TEDS $\uparrow$
MinerU2.5 (baseline)	93.23	91.65	92.98	—	0.045	95.59	87.88
Stage 1: Large-Scale SFT	94.54	93.10	94.29	+1.31	0.039	96.40	90.37
+ Stage 2: Hard-Sample SFT	95.60	93.84	95.25	+0.96	0.036	96.48	92.87
+ Stage 3: GRPO	<b>96.12</b>	<b>94.08</b>	<b>95.69</b>	+0.45	<b>0.036</b>	<b>97.29</b>	<b>93.42</b>

subset, the top three models (GLM-OCR 96.19, MinerU2.5-Pro 96.12, PaddleOCR-VL-1.5 95.72) are within 0.5 points, indicating near-saturation on standard scenarios. On the Hard subset, MinerU2.5-Pro leads at 94.08, exceeding both GLM-OCR and PaddleOCR-VL-1.5 (both at 92.01) by 2.07 points, demonstrating the Data Engine’s advantage in hard scenario robustness and validating the Hard subset’s discriminative power.

Across sub-metrics, MinerU2.5-Pro achieves the best scores in formula recognition (CDM 97.29), table recognition (TEDS 93.42, TEDS-S 95.92), and reading order (0.120). Notably, Gemini 3 Pro/Flash benefit substantially from the corrected matching in OmniDocBench v1.6 (Full 92.85/92.58), narrowing the gap with specialized models, yet specialized models at only 0.9B–1.2B parameters maintain an overall lead.

**Training stage ablation.** Table 3 reports the incremental contribution of each training stage.

Stage 1 (large-scale SFT) contributes the largest single-stage gain (+1.31), indicating that the Data Engine’s optimization of data coverage and annotation quality is the primary driver of performance improvement. Stage 2 (hard sample fine-tuning) adds +0.96, with the most notable contribution in table recognition (TEDS 90.37  $\rightarrow$  92.87, +2.50). Stage 3 (GRPO) contributes +0.45, primarily reflected in formula CDM improvement (96.48  $\rightarrow$  97.29, +0.81), driven by reinforcement learning’s direct optimization of task-level metrics. The cumulative improvement on the Hard subset (91.65  $\rightarrow$  94.08, +2.43) is comparable to the Base subset (93.23  $\rightarrow$  96.12, +2.89), indicating that the progressive training strategy achieves balanced capability improvement across both hard and standard scenarios.

Table 4: Text recognition (Edit Distance $\downarrow$ ) on OmniDocBench v1.6.

Model	Type	Base $\downarrow$	Hard $\downarrow$	Full $\downarrow$
<b>MinerU2.5-Pro</b>	Decoupled	<b>0.015</b>	<b>0.048</b>	<b>0.019</b>
Qwen3.5-397B [33]	General	<u>0.016</u>	0.052	<u>0.020</u>
GLM-OCR [11]	Decoupled	0.016	0.053	0.021
Qwen3-VL-235B [43]	General	0.017	<u>0.049</u>	0.021
PaddleOCR-VL-1.5 [8]	Decoupled	0.018	0.056	0.022
MinerU2.5 [25]	Decoupled	0.023	0.066	0.028
PaddleOCR-VL [6]	Decoupled	0.019	0.057	0.023
DeepSeek-OCR 2 [40]	End-to-End	0.057	0.130	0.066
FireRed-OCR [41]	End-to-End	0.135	0.176	0.140

Table 5: Formula recognition (CDM $\uparrow$ ) across multiple benchmarks. CPE, HWE, SCE, and SPE are the Complex Printed, Handwritten, Screen-Captured, and Simple Printed Expression subsets from UniMERNet [34], respectively.

Model	OmniDoc		Public					Inhouse	
	Base	Hard	CPE	HWE	SCE	SPE	LaTeX-80M	Chinese	Fuzzy
<b>MinerU2.5-Pro</b>	<b>99.20</b>	<b>98.79</b>	<b>98.97</b>	<u>95.38</u>	<u>97.04</u>	<b>99.44</b>	<b>97.23</b>	<u>95.28</u>	<u>94.90</u>
PaddleOCR-VL-1.5 [8]	<u>98.76</u>	97.22	98.84	92.27	94.95	99.27	92.77	94.06	89.73
GLM-OCR [11]	98.75	98.28	96.74	95.10	<b>97.77</b>	98.42	95.39	94.35	93.75
PaddleOCR-VL [6]	98.72	97.64	<u>98.93</u>	94.45	95.88	99.30	93.67	94.35	91.56
Qwen3.5-397B [33]	98.19	97.25	<u>98.32</u>	<b>97.59</b>	95.87	<u>99.41</u>	95.17	78.24	90.53
Qwen3-VL-235B [43]	97.72	98.13	97.47	94.23	96.21	98.46	95.33	92.69	93.59
MinerU2.5 [25]	97.25	<u>98.67</u>	97.79	94.42	96.65	98.57	<u>96.23</u>	<b>95.50</b>	<b>94.92</b>
FireRed-OCR [41]	96.71	94.54	94.35	85.42	89.94	96.75	83.41	87.94	87.77
DeepSeek-OCR 2 [40]	95.95	93.39	91.97	81.67	77.19	95.51	72.04	87.82	85.13

### 6.3 Element-Specific Parsing

Layout detection accuracy in end-to-end evaluation cascades into content recognition scores, and differences in output granularity and segmentation strategies across models prevent precise matching of a small number of elements. To more fairly evaluate pure content recognition capability, we crop document images based on ground truth layout boxes and test text, formula, and table recognition as individual modules. Note that end-to-end models do not receive element category priors in this setting, which may partially explain their larger performance gap compared to decoupled two-stage models.

**Text recognition.** As shown in Table 4, MinerU2.5-Pro ranks first on Full with an edit distance of 0.019, a 30.5% reduction from the MinerU2.5 baseline (0.028). Hundred-billion-scale general VLMs (Qwen3.5-397B, Qwen3-VL-235B) demonstrate competitive text recognition performance comparable to specialized models, while end-to-end models (DeepSeek-OCR 2, FireRed-OCR) show significant degradation without category priors.

**Formula recognition.** Table 5 reports CDM scores across 9 benchmarks. MinerU2.5-Pro achieves the best score in 5 dimensions and the second-highest in the remaining four. Specifically, it falls short on HWE (handwritten formulas) against Qwen3.5-397B (95.38 vs. 97.59) and on SCE against GLM-OCR (97.04 vs. 97.77), while only trailing slightly behind MinerU2.5 on Chinese and Fuzzy subsets. On OmniDocBench Base, CDM reaches 99.20 (out of 100), approaching the performance ceiling for formula recognition. While Qwen3.5-397B excels on handwritten formulas, it reveals a notable weakness on Chinese formulas (Chinese 78.24).

Table 6: Table recognition (TEDS & TEDS-S↑) across multiple benchmarks.

Model	Type	OmniDoc Base		OmniDoc Hard		CCOCR		OCRv2		Inhouse		Overall	
		TEDS	TEDS-S	TEDS	TEDS-S	TEDS	TEDS-S	TEDS	TEDS-S	TEDS	TEDS-S	TEDS	TEDS-S
MinerU2.5-Pro	Decoup.	<u>95.67</u>	<u>97.42</u>	<b>92.46</b>	<b>94.67</b>	88.49	<u>91.90</u>	<b>93.56</b>	<b>96.27</b>	<b>82.70</b>	<b>89.65</b>	<b>91.10</b>	<b>94.48</b>
GLM-OCR [11]	Decoup.	<b>96.14</b>	<b>97.60</b>	<u>90.49</u>	<u>93.47</u>	<b>89.17</b>	<b>92.58</b>	91.19	94.44	<u>79.41</u>	<u>87.65</u>	<u>89.71</u>	<u>93.52</u>
Gemini 3 Pro	General	94.42	97.37	88.16	91.34	86.47	90.10	91.73	94.96	75.91	85.26	88.21	92.65
PaddleOCR-VL-1.5 [8]	Decoup.	93.85	95.57	88.28	91.79	76.34	81.38	82.64	86.91	72.66	81.93	82.91	87.60
Qwen3.5-397B [33]	General	93.76	96.27	89.67	93.19	<u>88.87</u>	91.89	88.11	91.21	77.49	85.53	87.60	91.57
Qwen3-VL-235B [43]	General	92.92	95.48	87.55	91.80	87.38	91.22	88.81	92.94	74.39	83.94	86.64	91.44
MinerU2.5 [25]	Decoup.	92.87	95.33	88.28	91.80	84.35	88.25	<u>92.32</u>	<u>95.31</u>	76.95	85.98	87.94	92.17
PaddleOCR-VL [6]	Decoup.	92.31	94.64	89.21	92.02	81.54	85.80	82.29	85.79	74.88	82.92	83.67	87.85
FireRed-OCR [41]	E2E	88.12	90.29	86.11	89.58	82.24	86.62	86.93	90.34	69.57	79.02	83.02	87.47
DeepSeek-OCR 2 [40]	E2E	79.27	82.46	75.07	80.06	66.98	72.74	84.38	88.70	57.70	69.35	74.59	80.35

**Table recognition.** As shown in Table 6, MinerU2.5-Pro ranks first in both Overall TEDS (91.10) and TEDS-S (94.48), improving over MinerU2.5 by 3.16 and 2.31 percentage points, respectively. The advantage is most pronounced on the Hard subset (TEDS 92.46 *vs.* MinerU2.5’s 88.28, +4.18), indicating that the Data Engine’s hard sample mining and expert annotation contribute most to table recognition. GLM-OCR is slightly better on OmniDocBench Base (96.14) and CCOCR (89.17) but is less stable than MinerU2.5-Pro across benchmarks. PaddleOCR-VL-1.5 shows notable performance drops on CCOCR (TEDS 76.34) and Inhouse (TEDS 72.66), suggesting limited table recognition generalization.

## 7 Conclusion

We present MinerU2.5-Pro, which improves the OmniDocBench v1.6 overall score from 92.98 to 95.69 solely through systematic data engineering while keeping the 1.2B-parameter model architecture completely fixed, surpassing all existing methods. This result demonstrates that at the current stage where architectures are maturing, co-optimizing training data coverage, informativeness, and annotation accuracy yields greater performance gains than architectural improvements alone. To this end, we contribute a Data Engine that expands training data from under 10M to 65.5M pages while systematically improving annotation quality, a three-stage progressive training strategy matched to data quality tiers, and the OmniDocBench v1.6 three-tier evaluation protocol that corrects evaluation biases. These tools and methodologies provide the community with a performance improvement pathway that is orthogonal to and complementary with architectural innovation.

### Limitations and Future Directions

**Fundamental challenges in evaluation.** OmniDocBench v1.6 improves scoring fairness through corrected matching strategies, but the element-matching paradigm itself has inherent limitations. The ambiguity is twofold: at the format level, the same content can be expressed in multiple equivalent notations (*e.g.* HTML *vs.* Markdown for tables, different  $\LaTeX$  commands for the same formula); at the structural level, the same visual layout can be legitimately represented with different element types—for instance, a bilingual word list with aligned Chinese and English columns is equally valid as line-by-line text pairs or as a two-column table, and even human annotators may disagree on which representation is “correct.” Developing semantic-equivalence-aware evaluation methods that account for both format and structural ambiguity remains an open problem.

**Evaluation coverage and domain adaptation.** OmniDocBench v1.6 aims to cover mainstream application scenarios; for vertical domains with higher precision requirements (*e.g.* finance, legal, medical), constructing domain-specific evaluation sets is a necessary complement. Furthermore, as model capabilities approach human-level performance, ensuring the precision of evaluation set annotations themselves becomes an increasingly pressing challenge.

**From parsing accuracy to structural understanding.** This work focuses on content accuracy in document parsing. However, for downstream applications, structural relationships within documents—such as hierarchical relationships between headings and body text, semantic bindings between figures/tables and referring text, and cross-page content continuity—are equally critical for document retrieval and downstream semantic understanding. Advancing parsing from “content extraction” to “structured semantic understanding” represents a natural next step for document parsing research.

## References

- [1] Shuai Bai, Keqin Chen, Xuejing Liu, Jialin Wang, Wenbin Ge, Sibao Song, Kai Dang, Peng Wang, Shijie Wang, Jun Tang, et al. Qwen2. 5-vl technical report. *arXiv preprint arXiv:2502.13923*, 2025.
- [2] Lukas Blecher, Guillem Cucurull, Thomas Scialom, and Robert Stojnic. Nougat: Neural optical understanding for academic documents. *arXiv preprint arXiv:2308.13418*, 2023.
- [3] Song Chen, Xinyu Guo, Yadong Li, Tao Zhang, Mingan Lin, Dongdong Kuang, Youwei Zhang, Lingfeng Ming, Fengyu Zhang, Yuran Wang, et al. Ocean-ocr: Towards general ocr application via a vision-language model. *arXiv preprint arXiv:2501.15558*, 2025.
- [4] Xiangyang Chen, Shuzhao Li, Xiuwen Zhu, Yongfan Chen, Fan Yang, Cheng Fang, Lin Qu, Xiaoxiao Xu, Hu Wei, and Minggang Wu. Logics-parsing technical report, 2025. URL <https://arxiv.org/abs/2509.19760>.
- [5] Gheorghe Comanici, Eric Bieber, Mike Schaekermann, Ice Pasupat, Noveen Sachdeva, Inderjit Dhillon, Marcel Blistein, Ori Ram, Dan Zhang, Evan Rosen, et al. Gemini 2.5: Pushing the frontier with advanced reasoning, multimodality, long context, and next generation agentic capabilities. *arXiv preprint arXiv:2507.06261*, 2025.
- [6] Cheng Cui, Ting Sun, Suyin Liang, Tingquan Gao, Zelun Zhang, Jiaxuan Liu, Xueqing Wang, Changda Zhou, Hongen Liu, Manhui Lin, et al. Paddleocr-vl: Boosting multilingual document parsing via a 0.9 b ultra-compact vision-language model. *arXiv preprint arXiv:2510.14528*, 2025.
- [7] Cheng Cui, Ting Sun, Manhui Lin, Tingquan Gao, Yubo Zhang, Jiaxuan Liu, Xueqing Wang, Zelun Zhang, Changda Zhou, Hongen Liu, et al. Paddleocr 3.0 technical report. *arXiv preprint arXiv:2507.05595*, 2025.
- [8] Cheng Cui, Ting Sun, Suyin Liang, Tingquan Gao, Zelun Zhang, Jiaxuan Liu, Xueqing Wang, Changda Zhou, Hongen Liu, Manhui Lin, et al. Paddleocr-vl-1.5: Towards a multi-task 0.9 b vlm for robust in-the-wild document parsing. *arXiv preprint arXiv:2601.21957*, 2026.
- [9] Hejun Dong, Junbo Niu, Bin Wang, Weijun Zeng, Wentao Zhang, and Conghui He. Mineru-diffusion: Rethinking document ocr as inverse rendering via diffusion decoding. *arXiv preprint arXiv:2603.22458*, 2026.
- [10] Yongkun Du, Zhineng Chen, Yazhen Xie, Weikang Bai, Hao Feng, Wei Shi, Yuchen Su, Can Huang, and Yu-Gang Jiang. Unirec-0.1b: Unified text and formula recognition with 0.1b parameters. *arXiv preprint arXiv:2512.21095*, 2025.
- [11] Shuaiqi Duan, Yadong Xue, Weihang Wang, Zhe Su, Huan Liu, Sheng Yang, Guobing Gan, Guo Wang, Zihan Wang, Shengdong Yan, et al. Glm-ocr technical report. *arXiv preprint arXiv:2603.10910*, 2026.
- [12] Hao Feng, Shu Wei, Xiang Fei, Wei Shi, Yingdong Han, Lei Liao, Jinghui Lu, Binghong Wu, Qi Liu, Chunhui Lin, Jingqun Tang, Hao Liu, and Can Huang. Dolphin: Document image parsing via heterogeneous anchor prompting. In *Proceedings of the 65th Annual Meeting of the Association for Computational Linguistics (ACL)*, 2025.
- [13] Yoav Freund, H Sebastian Seung, Eli Shamir, and Naftali Tishby. Selective sampling using the query by committee algorithm. *Machine learning*, 28(2):133–168, 1997.
- [14] Samir Yitzhak Gadre, Gabriel Ilharco, Alex Fang, Jonathan Hayase, Georgios Smyrnis, Thao Nguyen, Ryan Marten, Mitchell Wortsman, Dhruva Ghosh, Jieyu Zhang, et al. Datacomp: In search of the next generation of multimodal datasets. *Advances in Neural Information Processing Systems*, 36:27092–27112, 2023.
- [15] Zirui Guo, Xubin Ren, Lingrui Xu, Jiahao Zhang, and Chao Huang. Rag-anything: All-in-one rag framework. *arXiv preprint arXiv:2510.12323*, 2025.
- [16] Geewook Kim, Teakgyu Hong, Moonbin Yim, Jinyoung Park, Jinyeong Yim, Wonseok Hwang, Sangdoon Yun, Dongyoon Han, and Seunghyun Park. Donut: Document understanding transformer without ocr. *arXiv preprint arXiv:2111.15664*, 7(15):2, 2021.
- [17] Vladimir I Levenshtein et al. Binary codes capable of correcting deletions, insertions, and reversals. In *Soviet physics doklady*, volume 10, pages 707–710. Soviet Union, 1966.
- [18] Yumeng Li, Guang Yang, Hao Liu, Bowen Wang, and Colin Zhang. dots. ocr: Multilingual document layout parsing in a single vision-language model. *arXiv preprint arXiv:2512.02498*, 2025.

- [19] Zhang Li, Yuliang Liu, Qiang Liu, Zhiyin Ma, Ziyang Zhang, Shuo Zhang, Zidun Guo, Jiarui Zhang, Xinyu Wang, and Xiang Bai. Monkeyocr: Document parsing with a structure-recognition-relation triplet paradigm. *arXiv preprint arXiv:2506.05218*, 2025.
- [20] Yuliang Liu, Zhang Li, Mingxin Huang, Biao Yang, Wenwen Yu, Chunyuan Li, Xu-Cheng Yin, Cheng-Lin Liu, Lianwen Jin, and Xiang Bai. Ocrbench: on the hidden mystery of ocr in large multimodal models. *Science China Information Sciences*, 67(12):220102, 2024.
- [21] Nikolaos Livathinos, Christoph Auer, Maksym Lysak, Ahmed Nassar, Michele Dolfi, Panos Vagenas, Cesar Berrospi Ramis, Matteo Omenetti, Kasper Dinkla, Yusik Kim, et al. Docling: An efficient open-source toolkit for ai-driven document conversion. *arXiv preprint arXiv:2501.17887*, 2025.
- [22] Shiyin Lu, Yang Li, Qing-Guo Chen, Zhao Xu, Weihua Luo, Kaifu Zhang, and Han-Jia Ye. Ovis: Structural embedding alignment for multimodal large language model, 2024. URL <https://arxiv.org/abs/2405.20797>.
- [23] Shiyin Lu, Yang Li, Yu Xia, Yuwei Hu, Shanshan Zhao, Yanqing Ma, Zhichao Wei, Yinglun Li, Lunhao Duan, Jianshan Zhao, Yuxuan Han, Haijun Li, Wanying Chen, Junke Tang, Chengkun Hou, Zhixing Du, Tianli Zhou, Wenjie Zhang, Huping Ding, Jiahe Li, Wen Li, Gui Hu, Yiliang Gu, Siran Yang, Jiamang Wang, Hailong Sun, Yibo Wang, Hui Sun, Jinlong Huang, Yuping He, Shengze Shi, Weihong Zhang, Guodong Zheng, Junpeng Jiang, Sensen Gao, Yi-Feng Wu, Sijia Chen, Yuhui Chen, Qing-Guo Chen, Zhao Xu, Weihua Luo, and Kaifu Zhang. Ovis2.5 technical report. *arXiv:2508.11737*, 2025.
- [24] Andrew Ng, Dillon Laird, and Lynn He. Data-centric ai competition. *DeepLearning AI. Available online: https://https-deeplearning-ai.github.io/data-centric-comp/(accessed on 9 December 2021)*, 2021.
- [25] Junbo Niu, Zheng Liu, Zhuangcheng Gu, Bin Wang, Linke Ouyang, Zhiyuan Zhao, Tao Chu, Tianyao He, Fan Wu, Qintong Zhang, Zhenjiang Jin, Guang Liang, Rui Zhang, Wenzheng Zhang, Yuan Qu, Zhifei Ren, Yuefeng Sun, Yuanhong Zheng, Dongsheng Ma, Zirui Tang, Boyu Niu, Ziyang Miao, Hejun Dong, Siyi Qian, Junyuan Zhang, Jingzhou Chen, Fangdong Wang, Xiaomeng Zhao, Liqun Wei, Wei Li, Shasha Wang, Ruiliang Xu, Yuanyuan Cao, Lu Chen, Qianqian Wu, Huaiyu Gu, Lindong Lu, Keming Wang, Dechen Lin, Guanlin Shen, Xuanhe Zhou, Linfeng Zhang, Yuhang Zang, Xiaoyi Dong, Jiaqi Wang, Bo Zhang, Lei Bai, Pei Chu, Weijia Li, Jiang Wu, Lijun Wu, Zhenxiang Li, Guangyu Wang, Zhongying Tu, Chao Xu, Kai Chen, Yu Qiao, Bowen Zhou, Dahua Lin, Wentao Zhang, and Conghui He. MinerU2.5: A decoupled vision-language model for efficient high-resolution document parsing. *arXiv preprint arXiv:2509.22186*, 2025.
- [26] Junbo Niu, Yuanhong Zheng, Ziyang Miao, Hejun Dong, Chunjiang Ge, Hao Liang, Ma Lu, Bohan Zeng, Qiahao Zheng, Conghui He, et al. Native visual understanding: Resolving resolution dilemmas in vision-language models. *arXiv preprint arXiv:2506.12776*, 2025.
- [27] Linke Ouyang, Yuan Qu, Hongbin Zhou, Jiawei Zhu, Rui Zhang, Qunshu Lin, Bin Wang, Zhiyuan Zhao, Man Jiang, Xiaomeng Zhao, et al. Omnidocbench: Benchmarking diverse pdf document parsing with comprehensive annotations. In *Proceedings of the IEEE/CVF Conference on Computer Vision and Pattern Recognition*, pages 24838–24848, 2025.
- [28] Vik Paruchuri. Marker. <https://github.com/datalab-to/marker>, 2025. Accessed:2025-09-25.
- [29] Jake Poznanski, Aman Rangapur, Jon Borchardt, Jason Dunkelberger, Regan Huff, Daniel Lin, Christopher Wilhelm, Kyle Lo, and Luca Soldaini. olmocr: Unlocking trillions of tokens in pdfs with vision language models. *arXiv preprint arXiv:2502.18443*, 2025.
- [30] H Sebastian Seung, Manfred Opper, and Haim Sompolinsky. Query by committee. In *Proceedings of the fifth annual workshop on Computational learning theory*, pages 287–294, 1992.
- [31] Zhihong Shao, Peiyi Wang, Qihao Zhu, Runxin Xu, Junxiao Song, Xiao Bi, Haowei Zhang, Mingchuan Zhang, YK Li, Yang Wu, et al. Deepseekmath: Pushing the limits of mathematical reasoning in open language models. *arXiv preprint arXiv:2402.03300*, 2024.
- [32] Hunyuan Vision Team, Pengyuan Lyu, Xingyu Wan, Gengluo Li, Shangpin Peng, Weinong Wang, Liang Wu, Huawen Shen, Yu Zhou, Canhui Tang, et al. Hunyuanocr technical report. *arXiv preprint arXiv:2511.19575*, 2025.

- [33] Qwen Team. Qwen3.5: Accelerating productivity with native multimodal agents, February 2026. URL <https://qwen.ai/blog?id=qwen3.5>.
- [34] Bin Wang, Zhuangcheng Gu, Guang Liang, Chao Xu, Bo Zhang, Botian Shi, and Conghui He. Unimernet: A universal network for real-world mathematical expression recognition. *arXiv preprint arXiv:2404.15254*, 2024.
- [35] Bin Wang, Chao Xu, Xiaomeng Zhao, Linke Ouyang, Fan Wu, Zhiyuan Zhao, Rui Xu, Kaiwen Liu, Yuan Qu, Fukai Shang, Bo Zhang, Liqun Wei, Zhihao Sui, Wei Li, Botian Shi, Yu Qiao, Dahua Lin, and Conghui He. Mineru: An open-source solution for precise document content extraction. *arXiv preprint arXiv:2409.18839*, 2024.
- [36] Bin Wang, Fan Wu, Linke Ouyang, Zhuangcheng Gu, Rui Zhang, Renqiu Xia, Botian Shi, Bo Zhang, and Conghui He. Image over text: Transforming formula recognition evaluation with character detection matching. In *Proceedings of the Computer Vision and Pattern Recognition Conference*, pages 19681–19690, 2025.
- [37] Shu Wang, Yingli Zhou, and Yixiang Fang. Bookrag: A hierarchical structure-aware index-based approach for retrieval-augmented generation on complex documents. *arXiv preprint arXiv:2512.03413*, 2025.
- [38] Weiyun Wang, Zhangwei Gao, Lixin Gu, Hengjun Pu, Long Cui, Xingguang Wei, Zhaoyang Liu, Linglin Jing, Shenglong Ye, Jie Shao, Zhaokai Wang, Zhe Chen, Hongjie Zhang, Ganlin Yang, Haomin Wang, Qi Wei, Jinhui Yin, Wenhao Li, Erfei Cui, Guanzhou Chen, Zichen Ding, Changyao Tian, Zhenyu Wu, Jingjing Xie, Zehao Li, Bowen Yang, Yuchen Duan, Xuehui Wang, Zhi Hou, Haoran Hao, Tianyi Zhang, Songze Li, Xiangyu Zhao, Haodong Duan, Nianchen Deng, Bin Fu, Yanan He, Yi Wang, Conghui He, Botian Shi, Junjun He, Yingtong Xiong, Han Lv, Lijun Wu, Wenqi Shao, Kaipeng Zhang, Huipeng Deng, Biqing Qi, Jiaye Ge, Qipeng Guo, Wenwei Zhang, Songyang Zhang, Maosong Cao, Junyao Lin, Kexian Tang, Jianfei Gao, Haiyan Huang, Yuzhe Gu, Chengqi Lyu, Huanze Tang, Rui Wang, Haijun Lv, Wanli Ouyang, Limin Wang, Min Dou, Xizhou Zhu, Tong Lu, Dahua Lin, Jifeng Dai, Weijie Su, Bowen Zhou, Kai Chen, Yu Qiao, Wenhao Wang, and Gen Luo. Internvl3.5: Advancing open-source multimodal models in versatility, reasoning, and efficiency, 2025. URL <https://arxiv.org/abs/2508.18265>.
- [39] Haoran Wei, Chenglong Liu, Jinyue Chen, Jia Wang, Lingyu Kong, Yanming Xu, Zheng Ge, Liang Zhao, Jianjian Sun, Yuang Peng, Chunrui Han, and Xiangyu Zhang. General ocr theory: Towards ocr-2.0 via a unified end-to-end model. *arXiv preprint arXiv:2409.01704*, 2024.
- [40] Haoran Wei, Yaofeng Sun, and Yukun Li. Deepseek-ocr: Contexts optical compression. *arXiv preprint arXiv:2510.18234*, 2025.
- [41] Hao Wu, Haoran Lou, Xinyue Li, Zuodong Zhong, Zhaojun Sun, Phellon Chen, Xuanhe Zhou, Kai Zuo, Yibo Chen, Xu Tang, Yao Hu, Boxiang Zhou, Jian Wu, Yongji Wu, Wenxin Yu, Yingmiao Liu, Yuhao Huang, Manjie Xu, Gang Liu, Yidong Ma, Zhichao Sun, and Changhao Qiao. Firered-ocr technical report, 2026. URL <https://arxiv.org/abs/2603.01840>.
- [42] Renqiu Xia, Song Mao, Xiangchao Yan, Hongbin Zhou, Bo Zhang, Haoyang Peng, Jiahao Pi, Daocheng Fu, Wenjie Wu, Hancheng Ye, et al. Docgenome: An open large-scale scientific document benchmark for training and testing multi-modal large language models. *arXiv preprint arXiv:2406.11633*, 2024.
- [43] An Yang, Anfeng Li, Baosong Yang, Beichen Zhang, Binyuan Hui, Bo Zheng, Bowen Yu, Chang Gao, Chengen Huang, Chenxu Lv, Chujie Zheng, Dayiheng Liu, Fan Zhou, Fei Huang, Feng Hu, Hao Ge, Haoran Wei, Huan Lin, Jialong Tang, Jian Yang, Jianhong Tu, Jianwei Zhang, Jianxin Yang, Jiayi Yang, Jing Zhou, Jingren Zhou, Junyang Lin, Kai Dang, Keqin Bao, Kexin Yang, Le Yu, Lianghao Deng, Mei Li, Mingfeng Xue, Mingze Li, Pei Zhang, Peng Wang, Qin Zhu, Rui Men, Ruize Gao, Shixuan Liu, Shuang Luo, Tianhao Li, Tianyi Tang, Wenbiao Yin, Xingzhang Ren, Xinyu Wang, Xinyu Zhang, Xuancheng Ren, Yang Fan, Yang Su, Yichang Zhang, Yinger Zhang, Yu Wan, Yuqiong Liu, Zekun Wang, Zeyu Cui, Zhenru Zhang, Zhipeng Zhou, and Zihan Qiu. Qwen3 technical report, 2025. URL <https://arxiv.org/abs/2505.09388>.
- [44] Zhibo Yang, Jun Tang, Zhaohai Li, Pengfei Wang, Jianqiang Wan, Humen Zhong, Xuejing Liu, Mingkun Yang, Peng Wang, Shuai Bai, et al. Cc-ocr: A comprehensive and challenging ocr benchmark for evaluating large multimodal models in literacy. In *Proceedings of the IEEE/CVF International Conference on Computer Vision*, pages 21744–21754, 2025.
- [45] Kun Yin, Yunfei Wu, Bing Liu, Zhongpeng Cai, Xiaotian Li, Huang Chen, Xin Li, Haoyu Cao, Yinsong Liu, Deqiang Jiang, Xing Sun, Yunsheng Wu, Qianyu Li, Antai Guo, Yanzhen Liao, Yanqiu Qu, Haodong Lin,

- Chengxu He, and Shuangyin Liu. Youtu-parsing: Perception, structuring and recognition via high-parallelism decoding, 2026. URL <https://arxiv.org/abs/2601.20430>.
- [46] Qiying Yu, Zheng Zhang, Ruofei Zhu, Yufeng Yuan, Xiaochen Zuo, Yu Yue, Weinan Dai, Tiantian Fan, Gaohong Liu, Lingjun Liu, et al. Dapo: An open-source llm reinforcement learning system at scale. *arXiv preprint arXiv:2503.14476*, 2025.
- [47] Daochen Zha, Zaid Pervaiz Bhat, Kwei-Herng Lai, Fan Yang, and Xia Hu. Data-centric ai: Perspectives and challenges. In *Proceedings of the 2023 SIAM international conference on data mining (SDM)*, pages 945–948. SIAM, 2023.
- [48] Junyuan Zhang, Qintong Zhang, Bin Wang, Linke Ouyang, Zichen Wen, Ying Li, Ka-Ho Chow, Conghui He, and Wentao Zhang. Ocr hinders rag: Evaluating the cascading impact of ocr on retrieval-augmented generation. In *Proceedings of the IEEE/CVF International Conference on Computer Vision*, pages 17443–17453, 2025.
- [49] Qintong Zhang, Bin Wang, Victor Shea-Jay Huang, Junyuan Zhang, Zhengren Wang, Hao Liang, Conghui He, and Wentao Zhang. Document parsing unveiled: Techniques, challenges, and prospects for structured information extraction. *arXiv preprint arXiv:2410.21169*, 2024.
- [50] Zhiyuan Zhao, Hengrui Kang, Bin Wang, and Conghui He. Doclayout-yolo: Enhancing document layout analysis through diverse synthetic data and global-to-local adaptive perception. *arXiv preprint arXiv:2410.12628*, 2024.
- [51] Xu Zhong, Elaheh ShafieiBavani, and Antonio Jimeno Yepes. Image-based table recognition: data, model, and evaluation. In *European conference on computer vision*, pages 564–580. Springer, 2020.
- [52] Yufeng Zhong, Lei Chen, Xuanle Zhao, Wenkang Han, Liming Zheng, Jing Huang, Deyang Jiang, Yilin Cao, Lin Ma, and Zhixiong Zeng. Ocrverse: Towards holistic ocr in end-to-end vision-language models, 2026. URL <https://arxiv.org/abs/2601.21639>.
- [53] Chunting Zhou, Pengfei Liu, Puxin Xu, Srinivasan Iyer, Jiao Sun, Yuning Mao, Xuezhe Ma, Avia Efrat, Ping Yu, Lili Yu, et al. Lima: Less is more for alignment. *Advances in Neural Information Processing Systems*, 36: 55006–55021, 2023.

# Appendix

## A Prompt Design and Task Examples

This section provides the prompt formats, output specifications, and representative examples for each task supported by MinerU2.5-Pro. All tasks share a unified prompt interface: a single `<image>` token followed by a plain-text task suffix, requiring no few-shot examples or structured metadata.

**Task Prompt Convention.** The five task suffixes and their output formats are summarized below:

- **Layout Detection** (§A.1) — localizes content regions and outputs bounding boxes with category labels and rotation flags.
- **Text Recognition** (§A.2) — transcribes cropped text regions into plain text.
- **Formula Recognition** (§A.3) — converts cropped formula regions into  $\text{\LaTeX}$  markup.
- **Table Recognition** (§A.4) — serializes cropped tables into an OTSL-based token sequence with cell content, subsequently converted to HTML.
- **Image Analysis** (§A.5) — classifies image regions and extracts captions and embedded content.

### A.1 Layout Detection

Layout Detection serves as the entry point of the document parsing pipeline, responsible for localizing all content regions on a page and assigning each a semantic category. The model takes a downsampled page image and produces a sequence of structured region descriptors.

#### Prompt.

`<image>\nLayout Detection:`

**Output Format.** The output is a newline-delimited sequence of region descriptors, where each region follows the format:

```
<|box_start|>x1 y1 x2 y2<|box_end|><|ref_start|>category<|ref_end|><|rotate_dir|>
```

Here, `x1 y1 x2 y2` are the normalized bounding box coordinates (scaled to a `[0, 999]` grid), `category` is the semantic label of the region (e.g., `title`, `text`, `header`, `footer`, `table`, `figure`, `formula`), and `<|rotate.dir|>` indicates the text orientation (`<|rotate_up|>` for standard upright text, with other directions for rotated content). Regions are emitted in natural reading order (top-to-bottom, left-to-right for left-to-right scripts).

**Example.** Given a document title page, the model outputs:

```
<|box_start|>705 112 899 146<|box_end|><|ref_start|>header<|ref_end|><|rotate_up|>
<|box_start|>030 343 132 397<|box_end|><|ref_start|>title<|ref_end|><|rotate_up|>
<|box_start|>212 330 491 382<|box_end|><|ref_start|>title<|ref_end|><|rotate_up|>
<|box_start|>214 389 767 441<|box_end|><|ref_start|>title<|ref_end|><|rotate_up|>
<|box_start|>219 494 359 523<|box_end|><|ref_start|>text<|ref_end|><|rotate_up|>
<|box_start|>654 940 907 975<|box_end|><|ref_start|>footer<|ref_end|><|rotate_up|>
```

This output identifies six regions—one header, three title blocks, one text block, and one footer—each with precise spatial coordinates and upright orientation. Additional examples are provided in [Figure 5](#).

## A.2 Text Recognition

Text Recognition transcribes cropped text regions into plain text. Each region is an original-resolution crop produced by Stage 1 Layout Detection.

### Prompt.

<image>\nText Recognition:

**Output Format.** The output is a plain-text string corresponding to the content of the cropped text region. No special tokens or markup are used—the model generates raw text as-is, including whitespace, punctuation, and any inline symbols present in the source image. Additional examples are provided in [Figure 6](#).

## A.3 Formula Recognition

Formula Recognition converts cropped formula regions into  $\LaTeX$  markup. The model supports both inline and display-style formulas, as well as multi-line equation environments.

### Prompt.

<image>\nFormula Recognition:

**Output Format.** The output is a  $\LaTeX$  math string. Display-style (block) formulas are wrapped in  $[. . .]$  delimiters. Equation numbers, when present in the source image, are preserved via  $\tag{. . .}$ . The model generates standard  $\LaTeX$  math commands and environments (e.g.,  $\frac$ ,  $\mathrm$ ,  $\quad$ ), ensuring the output is directly compilable.

**Example: Single Display Formula.** Given a cropped equation region, the model outputs:

$$[L = 0.004 \ln (2D/d) \quad (\mu \mathrm{H} / \mathrm{cm}) \tag{4-2-10}]$$

The equation number (4-2-10) from the original document is captured via  $\tag{\}$ .

**Multi-line Formulas.** Multi-line equations are handled through the collaboration of Layout Detection and Formula Recognition. Layout Detection first identifies an `equation.block` region encompassing the entire multi-line group, within which individual single-line formulas are separately localized. Each line is then independently cropped and recognized by Formula Recognition. The final multi-line output is produced by concatenating the individual  $\LaTeX$  results in reading order, faithfully reproducing the original equation group without requiring the model to generate multi-line environments in a single pass. Additional examples are provided in [Figure 7](#).

## A.4 Table Recognition

Table Recognition converts cropped table regions into a structured token sequence based on OTSL (Optimized Table Structure Language). Cell content is transcribed as plain text, with inline formulas in  $\LaTeX$  when present. The OTSL output is subsequently converted to HTML for downstream consumption.

### Prompt.

<image>\nTable Recognition:

**Output Format.** The output is a flat token sequence representing the table structure row by row. Each cell is delimited by `<fcel>`, and rows are separated by `<n1>`. Cell content may contain plain text,  $\LaTeX$  inline math (`\( . . . \)`), or a mixture of both. The OTSL representation is compact and unambiguous, supporting regular grids as well as cells with complex content. After generation, the OTSL sequence is programmatically converted to HTML for rendering and downstream integration.

**Example.** Given a cropped table with two rows (a header row of time values and a data row of concentration values), the model outputs:

```
<fcel>\( \frac{t}{\min} \)<fcel>3<fcel>5<fcel>7<fcel>10<fcel>15<fcel>21<fcel>25<n1>
<fcel>\( \frac{1/c}{\{\mathrm{\;}\{mol\}\}^{-1}\cdot \{\mathrm{\;}\{dm\}\}^3} \)<fcel>135.1
<fcel>157.7<fcel>181.8<fcel>215.5<fcel>275.5<fcel>347.2<fcel>393.2<n1>
```

Each `<fcel>` token introduces a cell, and `<n1>` marks the end of a row. The first column contains  $\LaTeX$ -formatted headers with units, while the remaining columns hold numeric values.

Additional examples are provided in [Figure 8](#).

### A.5 Image-Aware Parsing

Image Analysis classifies cropped image regions and extracts their embedded content. Unlike other recognition tasks that target a single modality, Image Analysis first determines the semantic type of the image and then extracts structured content accordingly—text, formulas, tables, or a combination thereof.

#### Prompt.

```
<image>\nImage Analysis:
```

**Output Format.** The output consists of four structured fields delimited by special tokens:

```
<|class_start|>class<|class_end|>
<|sub_class_start|>sub_class<|sub_class_end|>
<|caption_start|>caption<|caption_end|>
<|content_start|>content<|content_end|>
```

Here, `class` is the primary image category (e.g., `pure_formula`, `natural_image`, `chart`), `sub_class` provides a finer-grained label, `caption` captures any associated caption text (left empty if absent), and `content` contains the extracted textual or structured content from within the image.

**Example.** Given a cropped figure region containing a standalone formula, the model outputs:

```
<|class_start|>pure_formula<|class_end|>
<|sub_class_start|>pure_formula<|sub_class_end|>
<|caption_start|><|caption_end|>
<|content_start|>p + q = 1<|content_end|>
```

The image is classified as `pure_formula` with no caption, and the formula content is directly extracted. Additional examples are provided in [Figure 9](#).

## B Extended Parsing Capabilities

Beyond improvements in recognition accuracy, MinerU2.5-Pro extends the parsing capabilities of MinerU2.5 in several practical dimensions. These features target real-world deployment scenarios

where documents are multi-page, richly illustrated, and structurally complex. While they do not affect OmniDocBench scores (which focus on single-page content recognition), they substantially improve end-to-end parsing completeness and usability.

**Image-aware parsing.** MinerU2.5 crops all image regions without further processing, discarding potentially valuable information such as chart data, embedded text, and diagram content. MinerU2.5-Pro introduces image-aware parsing (§A.5) that first classifies each image region into fine-grained subtypes (chart, text image, table-like image, general image) and then applies differentiated extraction strategies: charts are parsed into structured tables, text images undergo OCR, and table-like images are recognized as tables. This framework is readily extensible to additional image types; however, we have not yet applied Data Engine optimization to image analysis data in this release, leaving significant room for future improvement.

**Truncated paragraph merging.** Layout Detection tends to segment each spatially distinct text block as an independent region, which can split semantically continuous paragraphs into multiple fragments. Common causes include column boundaries in multi-column layouts, figures or tables interrupting a paragraph, and unusually wide line spacing. To address this, MinerU2.5-Pro performs *truncated paragraph merging* as part of the Layout Detection task. Since Layout Detection already establishes reading order, and truncation necessarily occurs between consecutive regions in that order, the problem reduces to a binary classification at each adjacent-region boundary: *merge* or *no merge*. This binary label is integrated directly into the layout output sequence, allowing truncated paragraphs to be reassembled during final Markdown rendering without affecting downstream recognition tasks. The merging process is illustrated in [Figure 10](#).

To construct training data for this capability, we annotate merge decisions on top of existing layout ground truth. For each pair of adjacent text or `list_item` regions, we first apply rule-based filtering using sentence length, leading numbering patterns, and terminal punctuation to eliminate obvious non-merge cases. For the remaining candidates, we highlight the two regions in red and green on the page image and query Gemini 3 Flash with both the annotated image and the text content of each region, asking it to judge whether merging is appropriate based on layout context and textual coherence. To reduce API cost, only the first and last sentences are provided for long paragraphs.

**Cross-page table merging.** When a table is split across a page break, MinerU2.5-Pro automatically detects and merges the fragments. The system first applies rule-based heuristics to identify candidate pairs: if the last table on a page and the first table on the next page share compatible column counts and structural patterns, they are flagged for merging. For flagged pairs, the model receives the last row(s) of the upper table and the first data row(s) of the lower table as a structured text prompt:

Please merge the next two tables.

```
## Table 1 (Previous Page - Last Table)
**Last Row(s) Data:**
[[{content of table 1}]]
```

```
## Table 2 (Current Page - First Table)
**First Data Row(s):**
[[{content of table 2}]]
```

The model outputs a per-column binary decision list indicating whether each column should be *directly concatenated* (0) or *semantically merged* (1). Direct concatenation applies when cells are cleanly split at the page boundary (e.g. a single cell’s content is broken across two rows), while semantic merging preserves both rows as distinct data. A typical semantic merging process is shown in [Figure 11](#). This fine-grained,

column-level strategy handles the common case where some columns require concatenation and others do not within the same table split.

**In-table image detection.** Tables in real-world documents frequently contain embedded images (e.g., product photos, diagrams, icons). MinerU2.5-Pro detects these through a three-step process:

1. **Detection.** Layout Detection identifies image regions that fall spatially within a table bounding box. Each detected in-table image is replaced with a special placeholder token in the table crop, effectively masking the image region.
2. **Recognition.** The masked table image is fed to Table Recognition, which generates the OTSL sequence with placeholder tokens marking the positions of masked images.
3. **Restoration.** In the final output, placeholder tokens are resolved back to references to the original image regions, producing HTML table cells that contain `<img>` tags with unique identifiers linking to the extracted image content blocks.

This approach allows the table structure and textual content to be recognized without interference from embedded images, while preserving the spatial correspondence between images and their containing cells in the final output. Representative examples are shown in [Figure 12](#).

## C OmniDocBench v1.6 Detailed Results

This section reports per-model detailed results on the OmniDocBench v1.6 Base and Hard subsets. The evaluation protocol and matching corrections are described in [Section 5](#).

### C.1 Detailed Results on Base Subset

[Table 7](#) reports detailed evaluation results for all models on the OmniDocBench v1.6 Base subset.

On the Base subset, top model scores are tightly clustered: the top 6 Overall scores fall within 94.49–96.19, a range of only 1.70 points. MinerU2.5-Pro ranks second at 96.12, only 0.07 points behind GLM-OCR, while leading in Text Edit Distance (0.033 *vs.* 0.039), Table TEDS (94.49 *vs.* 94.36), and Reading Order (0.109 *vs.* 0.122).

### C.2 Detailed Results on Hard Subset

[Table 8](#) reports detailed evaluation results for all models on the OmniDocBench v1.6 Hard subset.

Rankings on the Hard subset differ markedly from Base, validating its effectiveness in differentiating model capabilities. Key observations: (1) MinerU2.5-Pro leads at 94.08, ahead of the second-place PaddleOCR-VL (92.48) by 1.60 points, achieving the best scores in Formula CDM (97.54), Table TEDS (89.91), and Reading Order (0.170). (2) GLM-OCR ranks first on Base (96.19) but drops to third on Hard (92.01), a decline of 4.18 points; HunyuanOCR drops from Base (92.45) to Hard (82.69), a decline of 9.76 points. In contrast, MinerU2.5-Pro declines by only 2.04 points, demonstrating the strongest robustness. (3) Gemini 3 Pro/Flash perform well on Hard (91.99), narrowing the gap with specialized models, benefiting from their strong capabilities on hard formulas (CDM 97.23/96.68).

## D Qualitative Comparison with SOTA Methods

This section presents qualitative comparisons of parsing results between MinerU2.5-Pro and current SOTA methods on representative scenarios.

Table 7: Detailed results on OmniDocBench v1.6 Base subset.

Model	Overall↑	Text Edit↓	Formula CDM↑	Table TEDS↑	TEDS-S↑	Read Order↓
<b>GLM-OCR</b>	<b>96.19</b>	0.039	<b>98.10</b>	94.36	96.59	0.122
MinerU2.5-Pro	96.12	<b>0.033</b>	97.16	<b>94.49</b>	<b>96.63</b>	<b>0.109</b>
PaddleOCR-VL-1.5	95.72	0.032	97.18	93.17	95.31	0.118
Youtu-Parsing	94.87	0.038	94.32	94.07	96.56	0.101
Ovis	94.56	0.031	95.11	91.64	94.33	0.125
PaddleOCR-VL	94.49	0.035	95.43	91.51	94.39	0.123
Logics-Parsing-v2	94.16	0.036	95.06	91.04	93.92	0.127
FireRed-OCR	94.14	0.030	95.63	89.76	92.41	0.120
MinerU2.5	93.23	0.042	94.81	89.06	92.24	0.120
OpenDoc-0.1B	93.04	0.039	94.05	88.93	91.99	0.126
Gemini 3 Pro	92.96	0.060	95.11	89.80	93.36	0.157
Gemini 3 Flash	92.58	0.062	94.19	89.74	93.82	0.163
HunyuanOCR	92.45	0.082	91.09	94.44	95.76	0.156
DeepSeek-OCR-2.0	91.50	0.046	93.02	86.13	89.75	0.134
dots.ocr	90.91	0.041	88.85	88.02	90.99	0.126
Dolphin-2.0	90.42	0.064	89.98	87.67	90.31	0.137
Qwen3-VL-235B	90.08	0.062	91.86	84.61	87.89	0.157
OCRverse	89.36	0.054	88.77	84.67	88.19	0.152
MonkeyOCR-pro-3B	89.15	0.067	86.87	87.22	90.49	0.181
Dolphin-1.5	87.24	0.091	86.32	84.47	87.55	0.157
GPT-5.2	86.83	0.120	88.62	83.82	88.31	0.188
Mistral-OCR	86.36	0.095	89.28	79.34	83.32	0.161
POINTS-Reader	86.20	0.095	89.69	78.37	81.43	0.184
Nanonets-OCR-s	86.10	0.099	86.43	81.75	85.41	0.192
olmOCR	85.89	0.135	87.00	84.17	87.64	0.205
InternVL 3.5	83.76	0.137	89.39	75.58	80.53	0.214

### D.1 Table Recognition

MinerU2.5-Pro demonstrates superior accuracy on complex tables, particularly rotated tables and tables with long merged cells. As shown in [Figure 13](#) and [Figure 14](#), MinerU2.5-Pro correctly recovers the table structure and content, while competing models exhibit noticeable structural errors such as misaligned rows and lost cell boundaries.

### D.2 Formula Recognition

The decoupled row-by-row formula analysis of MinerU2.5-Pro yields high accuracy on multi-line formulas, substantially outperforming end-to-end approaches that must generate entire equation groups in a single pass. MinerU2.5-Pro also achieves more accurate recognition on complex matrices. Representative comparisons are shown in [Figure 15](#) and [Figure 16](#).

### D.3 Image-Aware Parsing

MinerU2.5-Pro’s image-aware parsing extracts structured content from chart and diagram regions that other models typically leave as opaque image placeholders. [Figure 17](#) and [Figure 18](#) compare parsing results across different chart types.

Table 8: Detailed results on OmniDocBench v1.6 Hard subset.

Model	Overall↑	Text Edit↓	Formula CDM↑	Table TEDS↑	TEDS-S↑	Read Order↓
<b>MinerU2.5-Pro</b>	<b>94.08</b>	<b>0.052</b>	<b>97.54</b>	<b>89.91</b>	<b>93.61</b>	<b>0.170</b>
PaddleOCR-VL	92.48	0.066	96.24	87.84	91.60	0.189
GLM-OCR	92.01	0.066	94.81	87.81	91.44	0.186
PaddleOCR-VL-1.5	92.01	0.065	95.74	86.75	91.30	0.181
Gemini 3 Flash	91.99	0.085	96.68	87.83	92.51	0.214
Gemini 3 Pro	91.99	0.083	97.23	87.03	91.68	0.198
MinerU2.5	91.65	0.062	97.12	84.00	88.97	0.178
Ovis	90.39	0.056	94.56	82.21	86.07	0.184
Logics-Parsing-v2	89.95	0.062	96.28	79.81	85.61	0.184
FireRed-OCR	89.89	0.073	94.57	82.40	86.64	0.183
Youtu-Parsing	89.81	0.076	91.75	85.30	89.90	0.185
dots.ocr	88.67	0.081	89.65	84.42	89.25	0.196
Qwen3-VL-235B	88.45	0.065	93.85	78.01	83.00	0.210
DeepSeek-OCR-2.0	86.23	0.067	88.81	76.53	81.19	0.191
GPT-5.2	86.07	0.087	86.79	80.10	86.70	0.213
Dolphin-2.0	85.29	0.094	91.61	73.68	78.04	0.210
MonkeyOCR-pro-3B	85.07	0.109	91.18	74.92	82.48	0.228
OCRverse	84.79	0.106	89.86	75.11	79.99	0.215
olmOCR	84.34	0.157	89.58	79.17	85.65	0.269
InternVL 3.5	83.44	0.098	89.77	70.30	77.35	0.222
Dolphin-1.5	83.38	0.106	89.30	71.43	75.86	0.215
Mistral-OCR	82.85	0.104	90.62	68.36	73.08	0.219
OpenDoc-0.1B	82.69	0.100	90.73	67.32	72.55	0.206
HunyuanOCR	82.69	0.120	80.32	79.76	84.92	0.243
Nanonets-OCR-s	76.90	0.154	70.99	75.05	81.56	0.309
POINTS-Reader	74.86	0.103	75.23	59.60	64.19	0.263



Figure 5: Layout Detection examples. The model localizes content regions with bounding boxes, category labels, and rotation flags on diverse document pages.



Figure 6: Text Recognition examples across Chinese, English, and mixed-language text regions.

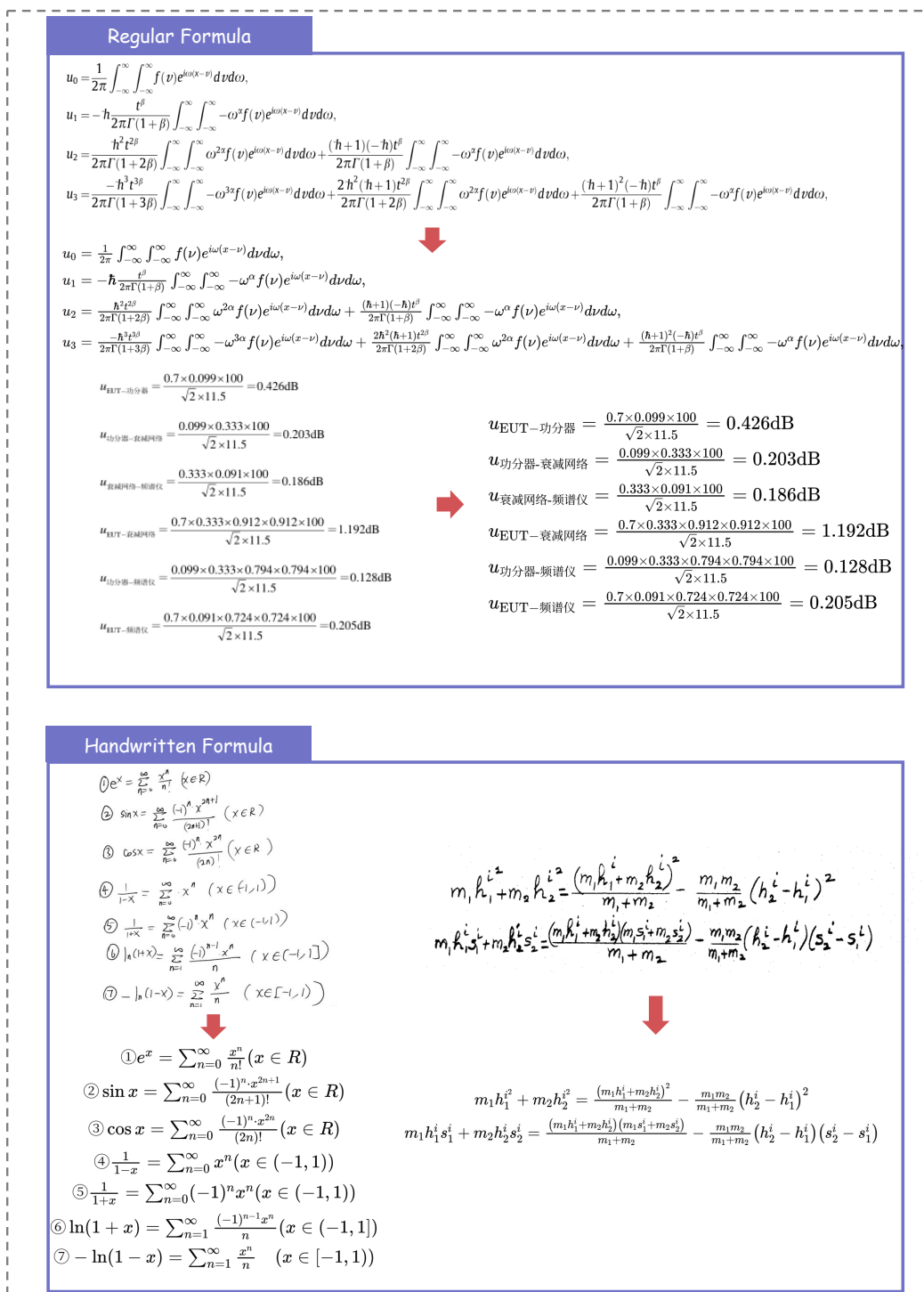


Figure 7: Formula Recognition examples including single-line display formulas and complex multi-line equations.

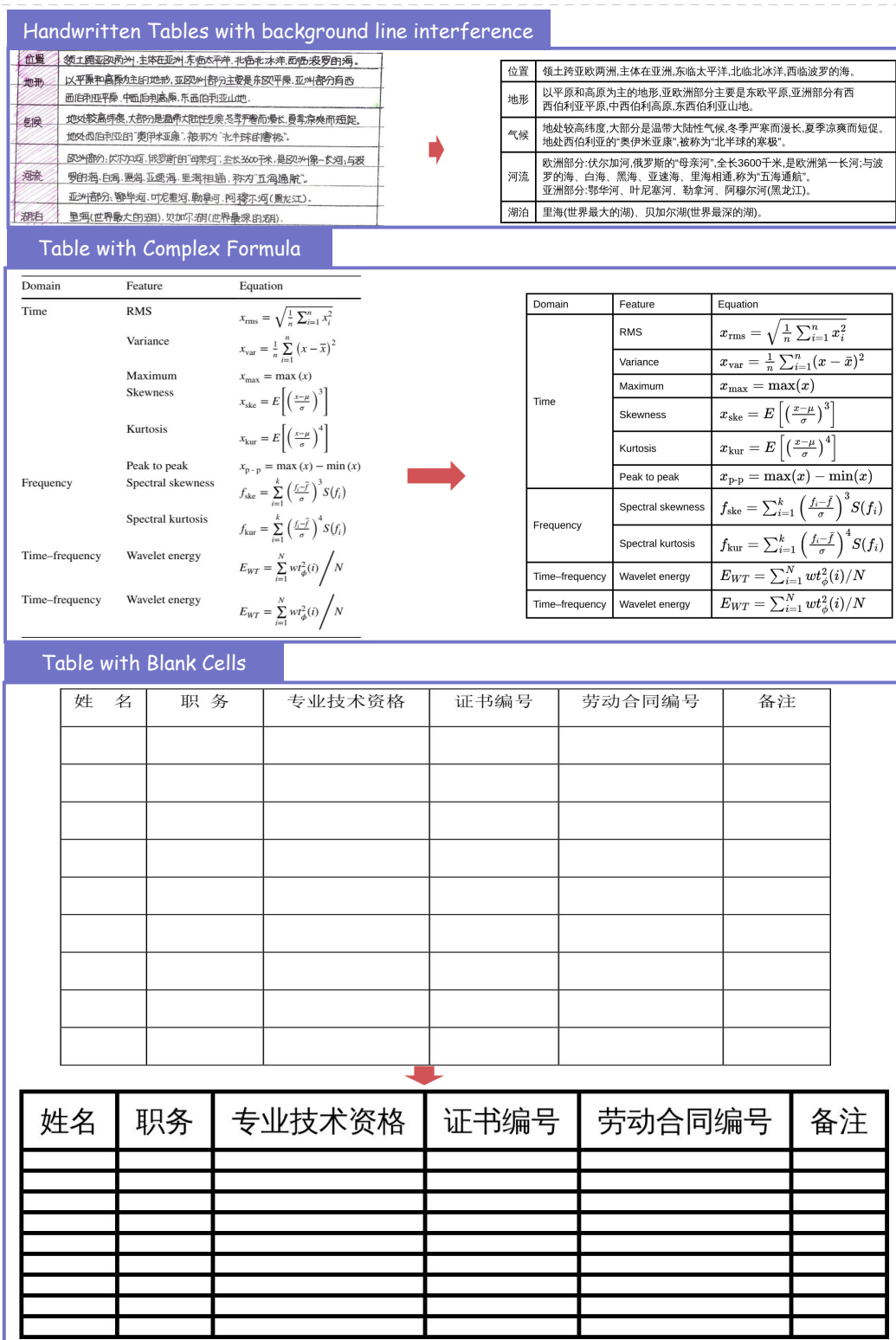


Figure 8: Table Recognition examples showing OTSL token output and the corresponding rendered HTML for tables with varying complexity.



Figure 9: Image-aware parsing examples. The model classifies image regions into fine-grained subtypes and extracts structured content accordingly.



Cross Page Table Recognition and Merging

pre-page table		next-page table	
		实际空载开度,观察机组转速上升平滑且不超过115%的额定转速 2.机组在额定转速运行一定时间后,待机组各轴承温度稳定无其他异常现象后,切换至自动位置,此时接力器应无明显摆动,在自动调节状态下,其相对转速摆动值不应超过0.20%	2、转速超过115%的额定转速扣5分; 3、未检查机组各轴承温度稳定无其他异常现象扣5分; 4、机组未稳定手动切换至自动位置扣5分;
5	空载扰动试验	1. 调速器调节器参数进行核对; 2. 设置一组调速器调节器参数 ( $K_p, K_i, K_d$ ), 观察空载稳定性与各项调节指标: a) 操作调速器电柜触摸屏,置频给为51.00Hz,机组稳定后置频给为49.00Hz,记录频率最低值、稳定时间、调节次数;稳定后将频给置51.00Hz,记录频率最高值、调节次数、稳定时间。 b) 操作调速器电柜触摸屏置频给恢复50.00Hz。 c) 操作调速器电柜触摸屏,置频给为52.00Hz,机组稳定后置频给为48.00Hz,记录频率最低值、稳定时间、调节次数;稳定后将频给置52.00Hz,记录频率最高值、调节次数、稳定时间。 d) 操作调速器电柜触摸屏置频给恢复50.00Hz。 3.重新一组调速器调节器参数,选择较好的调节参数 ( $K_p, K_i, K_d$ ),使调节品质达到最优,频率阶	33 1. 未调速器调节器参数不全扣3分; 2. 设置一组调速器调节器参数不全扣3分; 3. 未进行2%的频率上阶跃扣3分; 4. 未进行2%的频率下阶跃扣3分; 5. 未进行4%的频率上阶跃扣3分; 6. 未进行4%的频率下阶跃扣3分; 7. 未置频给恢复50.00Hz扣3分; 8. 选择调节参数,调节品质未达到频率变化衰减小于25%扣3分; 9. 选择调节参数,调节品质未达到频率最大超调量不超过扰动量 $\Delta f_0$ 的35%扣3分; 10. 选择调节参数,调节品质未达到调节时间 $T_p$ 不超过25s扣3分; 11. 选择调节参数,调节品质未达到调节时间内频差超过
6	试验完毕	注消工作票、拆除试验接线、清理现场	9 1.未注消工作票扣3分。 2.未拆除试验接线扣3分。 3.未清理现场扣3分。
7	试验数据记录及分析	1.试验数据应包括试验时间、天气、试验主要仪器及精度、试验数据、试验人等 2.出具分析报告	10 1. 试验数据不全每项扣1分扣完5分为止。 2. 无出具分析报告扣5分。
8 安全风险扣分项			
8.1	严重违章否定项	参照水电专业红线条款	/ 严重违章“一票否定”
8.2	其他违章扣分	参照水电专业红线条款	/ 一般违章按照10分/项次。
考试开始时间		考试结束时间	
考试成绩		合计扣分	
		考评员	
		考评组长	

		实际空载开度,观察机组转速上升平滑且不超过115%的额定转速 2.机组在额定转速运行一定时间后,待机组各轴承温度稳定无其他异常现象后,切换至自动位置,此时接力器应无明显摆动,在自动调节状态下,其相对转速摆动值不应超过0.20%	2、转速超过115%的额定转速扣5分;3、未检查机组各轴承温度稳定无其他异常现象扣5分;4、机组未稳定手动切换至自动位置扣5分;
5	空载扰动试验	1. 调速器调节器参数进行核对;2. 设置一组调速器调节器参数( $K_p, K_i, K_d$ ),观察空载稳定性与各项调节指标 a) 操作调速器电柜触摸屏,置频给为51.00Hz,机组稳定后置频给为49.00Hz,记录频率最低值、稳定时间、调节次数;稳定后将频给置51.00Hz,记录频率最高值、调节次数、稳定时间。 b) 操作调速器电柜触摸屏置频给恢复50.00Hz。 c) 操作调速器电柜触摸屏,置频给为52.00Hz,机组稳定后置频给为48.00Hz,记录频率最低值、稳定时间、调节次数;稳定后将频给置52.00Hz,记录频率最高值、调节次数、稳定时间。 d) 操作调速器电柜触摸屏置频给恢复50.00Hz。 3.重新一组调速器调节器参数,选择较好的调节参数 ( $K_p, K_i, K_d$ ),使调节品质达到最优,频率阶跃变化4%的调速器调节品质要求: a)频率变化衰减小于25%;b)频率最大超调量不超过扰动量 $\Delta f_0$ 的35%;c)由扰动开始,到调节稳定为止的调节时间 $T_p$ 不超过25s;d)在调节时间 $T_p$ 内,频差超过 $\pm 0.35\text{Hz}$ 的波动次数不超过两次。	33 1.未调速器调节器参数进行核对扣3分;2.设置一组调速器调节器参数不全扣3分;3.未进行2%的频率上阶跃扣3分;4.未进行2%的频率下阶跃扣3分;5.未进行4%的频率上阶跃扣3分;6.未进行4%的频率下阶跃扣3分;7.未置频给恢复50.00Hz扣3分;8.选择调节参数,调节品质未达到频率变化衰减小于25%扣3分;9.选择调节参数,调节品质未达到频率最大超调量不超过扰动量 $\Delta f_0$ 的35%扣3分;10.选择调节参数,调节品质未达到调节时间 $T_p$ 不超过25s扣3分;11.选择调节参数,调节品质未达到调节时间内频差超过 $\pm 0.35\text{Hz}$ 的波动次数不超过两次扣3分。
6	试验完毕	注消工作票、拆除试验接线、清理现场	9 1.未注消工作票扣3分。2.未拆除试验接线扣3分。3.未清理现场扣3分。
7	试验数据记录及分析	1.试验数据应包括试验时间、天气、试验主要仪器及精度、试验数据、试验人等 2.出具分析报告	10 1. 试验数据不全每项扣1分扣完5分为止。 2. 无出具分析报告扣5分。
8 安全风险扣分项			
8.1	严重违章否定项	参照水电专业红线条款	/ 严重违章“一票否定”
8.2	其他违章扣分	参照水电专业红线条款	/ 一般违章按照10分/项次。
考试开始时间		考试结束时间	
考试成绩		合计扣分	
		考评员	
		考评组长	

Figure 11: Cross-page table merging example. The model performs semantic understanding at the junction of two table fragments identified by rule-based heuristics, producing per-column merge decisions to reconstruct the complete table.

# MinerU2.5-Pro: Pushing the Limits of Data-Centric Document Parsing at Scale



Figure 12: In-table image detection and recognition. Embedded images within table cells are masked with placeholders during Table Recognition and restored as <img> references in the final HTML output.

# MinerU2.5-Pro: Pushing the Limits of Data-Centric Document Parsing at Scale

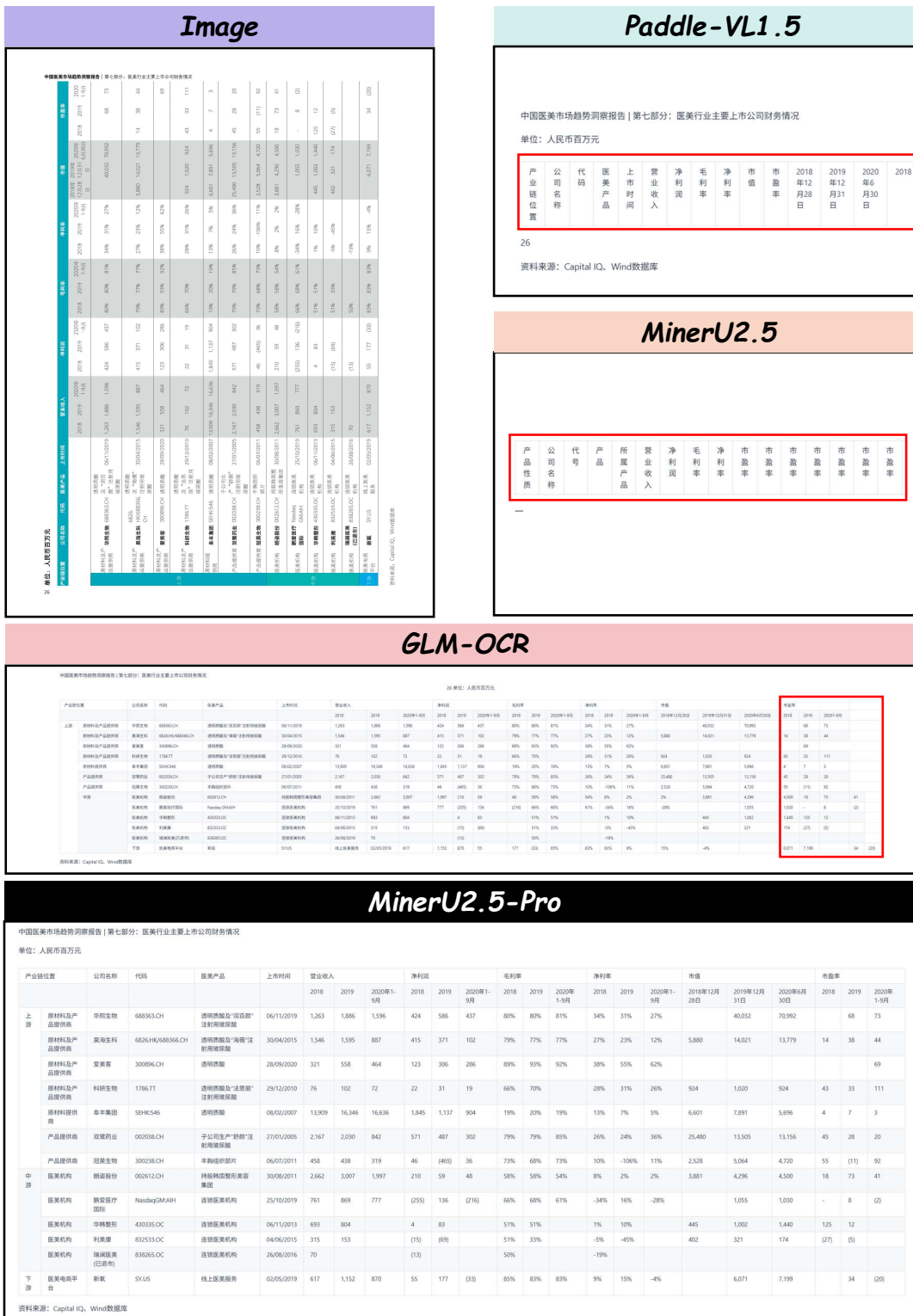


Figure 13: Qualitative comparison on rotated table recognition. MinerU2.5-Pro correctly recovers the rotated structure, while competing models produce misaligned rows or missing cells.

# MinerU2.5-Pro: Pushing the Limits of Data-Centric Document Parsing at Scale

**Image**

**Reference Only**

Spec. No. JENF43A-000A-01 P.2/12

Customer Part Number	MURATA Part Number	Impedance (Z) (at 100MHz, Under Standard Testing Conditions)	Rated Current (mA) (at 125°C)	DC Resistance (Ω) (at 20°C)	Value After Testing	Remark
	BLM18AG121SN1D	120±25%	120	800	0.18	For general use
	BLM18AG131SN1B	120±25%	120	800	0.18	
	BLM18AG141SN1B	150±25%	150	700	0.25	
	BLM18AG151SN1B	150±25%	150	700	0.25	
	BLM18AG211SN1B	220±25%	220	700	0.25	
	BLM18AG311SN1B	330±25%	330	600	0.30	
	BLM18AG411SN1B	470±25%	470	550	0.35	
	BLM18AG471SN1B	470±25%	470	550	0.35	
	BLM18AG601SN1D	600±25%	600	500	0.38	
	BLM18AG601SN1B	600±25%	600	500	0.38	
	BLM18AG100SN1B	1000±25%	1000	450	0.50	
	BLM18B000SN1D	5±25%	5	800	0.05	For high speed signal line
	BLM18B000SN1B	5±25%	5	800	0.05	
	BLM18B050SN1D	5±25%	5	500	0.2	
	BLM18B050SN1B	5±25%	5	500	0.2	
	BLM18B100SN1D	10±25%	10	700	0.10	
	BLM18B100SN1B	10±25%	10	500	0.25	
	BLM18B200SN1D	10±25%	10	700	0.20	
	BLM18B200SN1B	22±25%	22	500	0.35	
	BLM18B470SN1D	47±25%	47	600	0.25	
	BLM18B470SN1B	47±25%	47	500	0.3	
	BLM18B700SN1D	47±25%	47	300	0.55	
	BLM18B700SN1B	60±25%	60	600	0.25	
	BLM18B750SN1D	75±25%	75	300	0.70	
	BLM18B750SN1B	75±25%	75	600	0.30	
	BLM18B121SN1D	120±25%	120	550	0.30	
	BLM18B121SN1B	120±25%	120	300	0.4	
	BLM18B151SN1D	150±25%	150	300	0.9	
	BLM18B151SN1B	140±25%	140	500	0.35	
	BLM18B151SN1D	150±25%	150	450	0.37	
	BLM18B151SN1B	150±25%	150	300	0.4	
	BLM18B221SN1D	220±25%	220	450	0.45	
	BLM18B221SN1B	220±25%	220	250	0.45	
	BLM18B221SN1D	220±25%	220	250	0.45	
	BLM18B221SN1B	220±25%	220	250	0.45	

MURATA MFG.CO., LTD.

**MinerU2.5-Pro**

Reference Only  
Spec. No. JENF43A-000A-01  
P.2/12

Customer Part Number	MURATA Part Number	Impedance (Z) (at 100MHz, Under Standard Testing Conditions)	Rated Current (mA) (at 125°C)	DC Resistance (Ω) (at 20°C)	Value After Testing	Remark
	BLM18AG121SN1D	120±25%	120	800	0.18	For general use
	BLM18AG131SN1B	120±25%	120	800	0.18	
	BLM18AG141SN1B	150±25%	150	700	0.25	
	BLM18AG151SN1B	150±25%	150	700	0.25	
	BLM18AG211SN1B	220±25%	220	700	0.25	
	BLM18AG311SN1B	330±25%	330	600	0.30	
	BLM18AG411SN1B	470±25%	470	550	0.35	
	BLM18AG471SN1B	470±25%	470	550	0.35	
	BLM18AG601SN1D	600±25%	600	500	0.38	
	BLM18AG601SN1B	600±25%	600	500	0.38	
	BLM18B000SN1D	5±25%	5	800	0.05	For high speed signal line
	BLM18B000SN1B	5±25%	5	800	0.05	
	BLM18B050SN1D	5±25%	5	500	0.2	
	BLM18B050SN1B	5±25%	5	500	0.2	
	BLM18B100SN1D	10±25%	10	700	0.10	
	BLM18B100SN1B	10±25%	10	500	0.25	
	BLM18B200SN1D	10±25%	10	700	0.20	
	BLM18B200SN1B	22±25%	22	500	0.35	
	BLM18B470SN1D	47±25%	47	600	0.25	
	BLM18B470SN1B	47±25%	47	500	0.3	
	BLM18B700SN1D	47±25%	47	300	0.55	
	BLM18B700SN1B	60±25%	60	600	0.25	
	BLM18B750SN1D	75±25%	75	300	0.70	
	BLM18B750SN1B	75±25%	75	600	0.30	
	BLM18B121SN1D	120±25%	120	550	0.30	
	BLM18B121SN1B	120±25%	120	300	0.4	
	BLM18B151SN1D	150±25%	150	300	0.9	
	BLM18B151SN1B	140±25%	140	500	0.35	
	BLM18B151SN1D	150±25%	150	450	0.37	
	BLM18B151SN1B	150±25%	150	300	0.4	
	BLM18B221SN1D	220±25%	220	450	0.45	
	BLM18B221SN1B	220±25%	220	250	0.45	
	BLM18B221SN1D	220±25%	220	250	0.45	
	BLM18B221SN1B	220±25%	220	250	0.45	

MURATA MFG.CO., LTD.

**Paddle-VL1.5**

Reference Only  
Spec. No. JENF43A-000A-01  
P.2/12

Customer Part Number	MURATA Part Number	Impedance (Z) (at 100MHz, Under Standard Testing Conditions)	Rated Current (mA) (at 125°C)	DC Resistance (Ω) (at 20°C)	Value After Testing	Remark
	BLM18AG121SN1D	120±25%	120	800	0.18	For general use
	BLM18AG131SN1B	120±25%	120	800	0.18	
	BLM18AG141SN1B	150±25%	150	700	0.25	
	BLM18AG151SN1B	150±25%	150	700	0.25	
	BLM18AG211SN1B	220±25%	220	700	0.25	
	BLM18AG311SN1B	330±25%	330	600	0.30	
	BLM18AG411SN1B	470±25%	470	550	0.35	
	BLM18AG471SN1B	470±25%	470	550	0.35	
	BLM18AG601SN1D	600±25%	600	500	0.38	
	BLM18AG601SN1B	600±25%	600	500	0.38	
	BLM18B000SN1D	5±25%	5	800	0.05	For high speed signal line
	BLM18B000SN1B	5±25%	5	800	0.05	
	BLM18B050SN1D	5±25%	5	500	0.2	
	BLM18B050SN1B	5±25%	5	500	0.2	
	BLM18B100SN1D	10±25%	10	700	0.10	
	BLM18B100SN1B	10±25%	10	500	0.25	
	BLM18B200SN1D	10±25%	10	700	0.20	
	BLM18B200SN1B	22±25%	22	500	0.35	
	BLM18B470SN1D	47±25%	47	600	0.25	
	BLM18B470SN1B	47±25%	47	500	0.3	
	BLM18B700SN1D	47±25%	47	300	0.55	
	BLM18B700SN1B	60±25%	60	600	0.25	
	BLM18B750SN1D	75±25%	75	300	0.70	
	BLM18B750SN1B	75±25%	75	600	0.30	
	BLM18B121SN1D	120±25%	120	550	0.30	
	BLM18B121SN1B	120±25%	120	300	0.4	
	BLM18B151SN1D	150±25%	150	300	0.9	
	BLM18B151SN1B	140±25%	140	500	0.35	
	BLM18B151SN1D	150±25%	150	450	0.37	
	BLM18B151SN1B	150±25%	150	300	0.4	
	BLM18B221SN1D	220±25%	220	450	0.45	
	BLM18B221SN1B	220±25%	220	250	0.45	
	BLM18B221SN1D	220±25%	220	250	0.45	
	BLM18B221SN1B	220±25%	220	250	0.45	

MURATA MFG.CO., LTD.

**GLM-OCR**

Reference Only  
Spec. No. JENF43A-000A-01  
P.2/12

Customer Part Number	MURATA Part Number	Impedance (Z) (at 100MHz, Under Standard Testing Conditions)	Rated Current (mA) (at 125°C)	DC Resistance (Ω) (at 20°C)	Value After Testing	Remark
	BLM18AG121SN1D	120±25%	120	800	0.18	For general use
	BLM18AG131SN1B	120±25%	120	800	0.18	
	BLM18AG141SN1B	150±25%	150	700	0.25	
	BLM18AG151SN1B	150±25%	150	700	0.25	
	BLM18AG211SN1B	220±25%	220	700	0.25	
	BLM18AG311SN1B	330±25%	330	600	0.30	
	BLM18AG411SN1B	470±25%	470	550	0.35	
	BLM18AG471SN1B	470±25%	470	550	0.35	
	BLM18AG601SN1D	600±25%	600	500	0.38	
	BLM18AG601SN1B	600±25%	600	500	0.38	
	BLM18B000SN1D	5±25%	5	800	0.05	For high speed signal line
	BLM18B000SN1B	5±25%	5	800	0.05	
	BLM18B050SN1D	5±25%	5	500	0.2	
	BLM18B050SN1B	5±25%	5	500	0.2	
	BLM18B100SN1D	10±25%	10	700	0.10	
	BLM18B100SN1B	10±25%	10	500	0.25	
	BLM18B200SN1D	10±25%	10	700	0.20	
	BLM18B200SN1B	22±25%	22	500	0.35	
	BLM18B470SN1D	47±25%	47	600	0.25	
	BLM18B470SN1B	47±25%	47	500	0.3	
	BLM18B700SN1D	47±25%	47	300	0.55	
	BLM18B700SN1B	60±25%	60	600	0.25	
	BLM18B750SN1D	75±25%	75	300	0.70	
	BLM18B750SN1B	75±25%	75	600	0.30	
	BLM18B121SN1D	120±25%	120	550	0.30	
	BLM18B121SN1B	120±25%	120	300	0.4	
	BLM18B151SN1D	150±25%	150	300	0.9	
	BLM18B151SN1B	140±25%	140	500	0.35	
	BLM18B151SN1D	150±25%	150	450	0.37	
	BLM18B151SN1B	150±25%	150	300	0.4	
	BLM18B221SN1D	220±25%	220	450	0.45	
	BLM18B221SN1B	220±25%	220	250	0.45	
	BLM18B221SN1D	220±25%	220	250	0.45	
	BLM18B221SN1B	220±25%	220	250	0.45	

MURATA MFG.CO., LTD.

Figure 14: Qualitative comparison on tables with long merged cells. MinerU2.5-Pro preserves the span structure, whereas other models incorrectly split or duplicate merged cells.

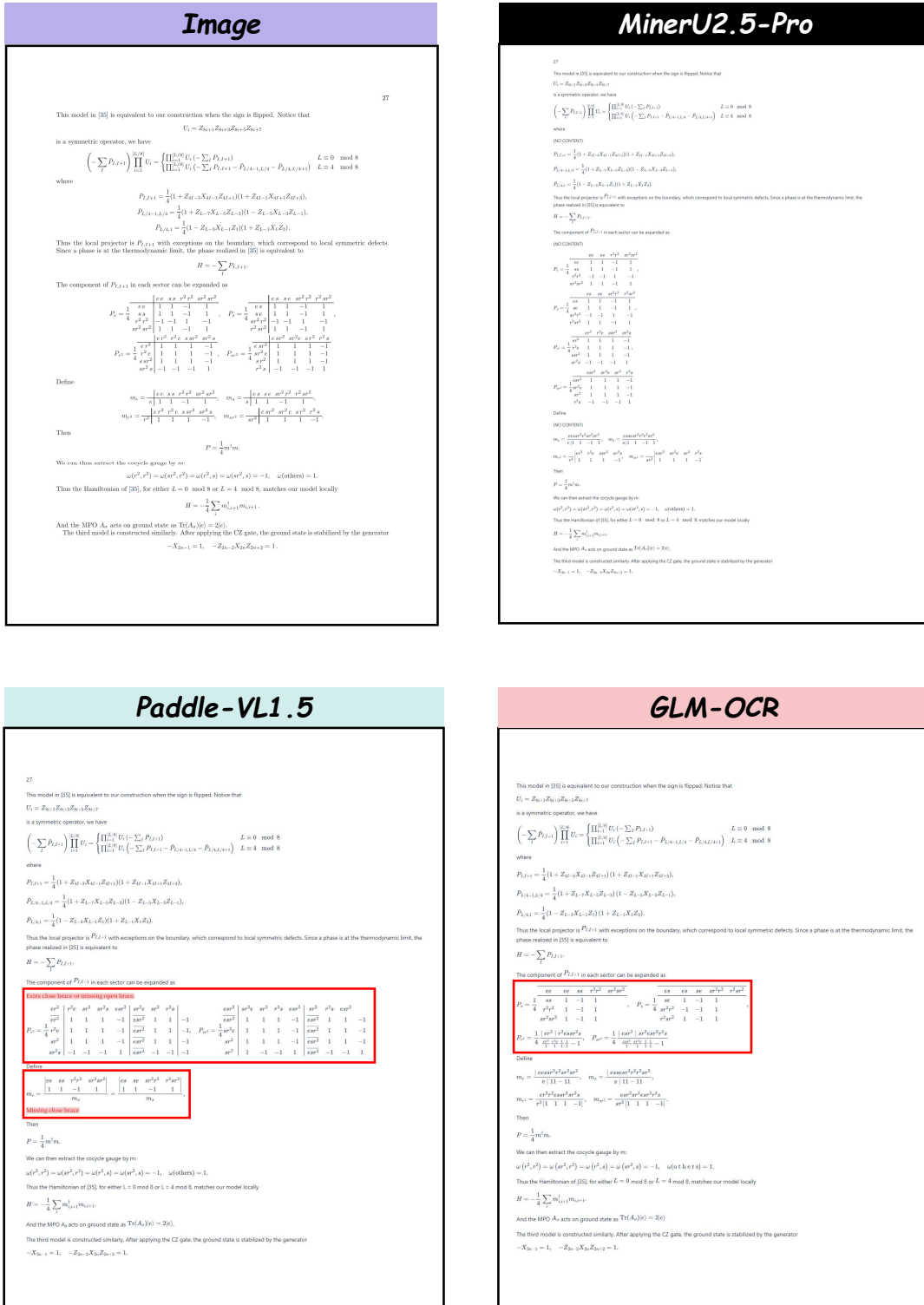


Figure 15: Qualitative comparison on complex matrix recognition. MinerU2.5-Pro accurately captures the matrix structure and alignment, while other models exhibit symbol errors or structural collapse.

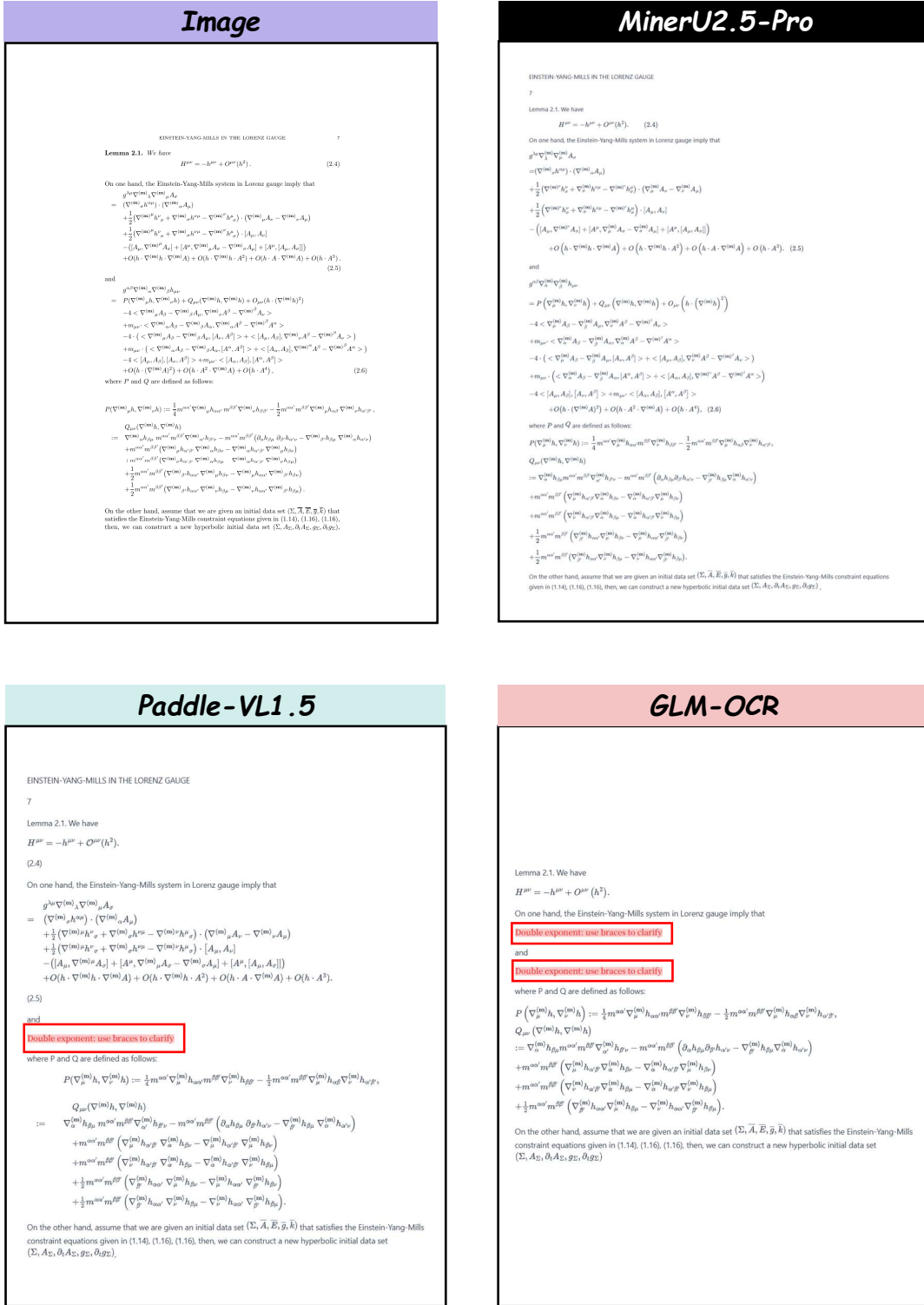


Figure 16: Qualitative comparison on multi-line formula recognition. The row-by-row analysis of MinerU2.5-Pro faithfully reproduces each line, whereas competing models merge or misalign lines.

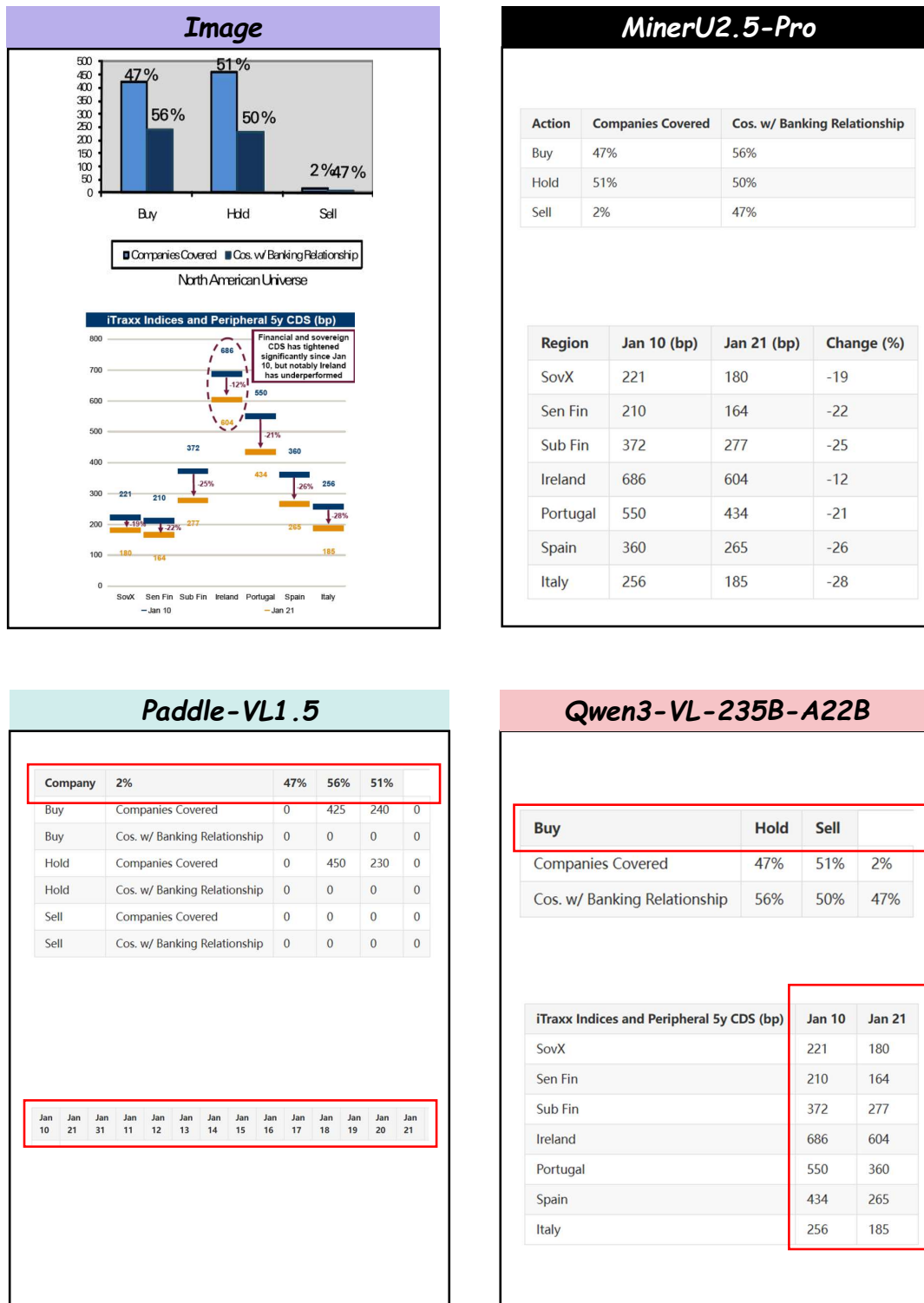
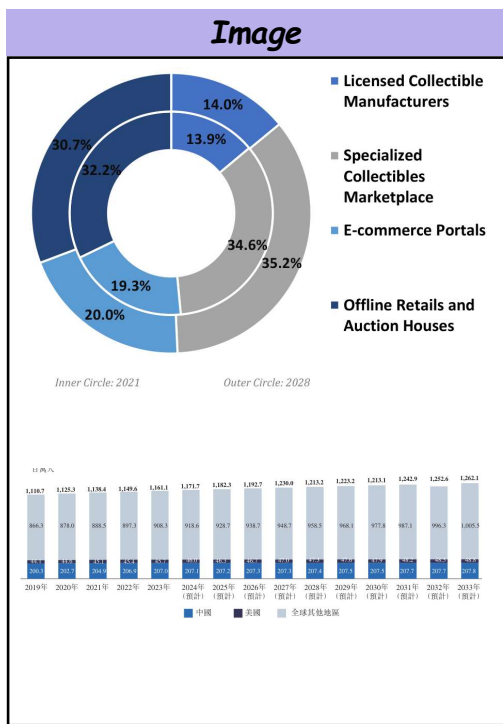


Figure 17: Qualitative comparison on image-aware chart parsing (Part 1). MinerU2.5-Pro extracts structured content from diverse chart types, while other models either ignore or misinterpret chart content.



### MinerU2.5-Pro

Category	Inner Circle: 2021 (%)	Outer Circle: 2028 (%)
Licensed Collectible Manufacturers	13.9	14.0
Specialized Collectibles Marketplace	34.6	35.2
E-commerce Portals	19.3	20.0
Offline Retailers and Auction Houses	30.7	32.2

年份	中國 (百萬人)	美國 (百萬人)	全球其他地區 (百萬人)
2019年	200.3	44.1	866.3
2020年	202.7	44.6	878.0
2021年	204.9	45.1	888.5
2022年	206.9	45.4	897.3
2023年	207.0	45.7	908.3
2024年 (預計)	207.1	46.0	918.6
2025年 (預計)	207.2	46.3	928.7
2026年 (預計)	207.3	46.7	938.7
2027年 (預計)	207.3	47.0	948.7
2028年 (預計)	207.4	47.3	958.5
2029年 (預計)	207.5	47.6	968.1
2030年 (預計)	207.5	47.9	977.8
2031年 (預計)	207.7	48.2	987.1
2032年 (預計)	207.7	48.3	996.3
2033年 (預計)	207.8	48.8	1,005.5

### Paddle-VL1.5

Category	Percentage (%)
Licensed Collectible Manufacturers	14.0
Specialized Collectibles Marketplace	34.6
E-commerce Portals	35.2
Inner Circle: 2021	32.2
Outer Circle: 2028	13.9

年份	中國	美國	全球其他地區
2019年	1110.7	866.3	44.1
2020年	1125.3	878.0	44.6
2021年	1138.4	888.5	45.1
2022年	1149.6	897.3	45.4
2023年	1161.1	908.3	45.7
2024年 (預計)	1171.7	918.6	46.0
2025年 (預計)	1182.3	928.7	46.3
2026年 (預計)	1192.7	938.7	46.7
2027年 (預計)	1230.0	948.7	47.0
2028年 (預計)	1213.2	958.5	47.3
2029年 (預計)	1223.2	968.1	47.6
2030年 (預計)	1213.1	977.8	47.9
2031年 (預計)	1242.9	987.1	48.2
2032年 (預計)	1252.6	996.3	48.5
2033年 (預計)	1262.1	1005.5	48.8

### Qwen3-VL-235B-A22B

Channel	2021 (%)	2028 (%)
Licensed Collectible Manufacturers	13.9	14.0
Specialized Collectibles Marketplace	34.6	35.2
E-commerce Portals	19.3	20.0
Offline Retailers and Auction Houses	32.2	30.7

年份	中國	美國	全球其他地區
2019年	200.3	44.1	866.3
2020年	202.7	44.6	878.0
2021年	204.9	45.1	888.5
2022年	206.9	45.4	897.3
2023年	207.0	45.7	908.3
2024年 (預計)	207.1	46.0	918.6
2025年 (預計)	207.2	46.3	928.7
2026年 (預計)	207.3	46.7	938.7
2027年 (預計)	207.3	47.0	948.7
2028年 (預計)	207.4	47.3	958.5
2029年 (預計)	207.5	47.6	968.1
2030年 (預計)	207.5	47.9	977.8
2031年 (預計)	207.7	48.2	987.1
2032年 (預計)	207.7	48.5	996.3
2033年 (預計)	207.8	48.8	1,005.5

Figure 18: Qualitative comparison on image-aware chart parsing (Part 2). Additional chart types demonstrating the generalization of MinerU2.5-Pro’s image analysis pipeline.